2D NAPL experiments using the CU γ-radiation system

H. Coumoulos, C. Kechavarzi,
K. Soga and T. Illangasekare

CUED/D-SOIL/TR309 (Jan. 1999)

INTRODUCTION

Under the collaboration between The University of Cambridge and The University of Colorado at Boulder, sand tank experiments of NAPL migration were conducted by two members of the Cambridge University Engineering Department using the facility in the Groundwater Laboratory of the University of Colorado at Boulder. The experiments lasted one month between November and December, 1997.

The primary aim of the experiments was:

(a) to use the facilities and the expertise developed over years of research at the laboratory of the University of Colorado at Boulder,

(b) to become familiar with the γ-rays attenuation system, and

(c) to perform NAPL migration tests using the facilities available there.

Two types of experiments were conducted; (a) one spill of LNAPL in a homogeneous unsaturated loamy sand and (b) two spills of DNAPL on saturated medium sand matrix incorporating an inclined coarser layer. A brief summary of the experiments is described as follows.

LNAPL experiment in a loamy sand

The aim of the experiment was to observe the migration of a lighter than water non-aqueous phase liquid (LNAPL) in a porous medium of a finer texture than the sand media commonly used in the literature. A two-dimensional LNAPL spill was conducted in a homogeneous unsaturated loamy sand. The soil was obtained by mixing a fine sand with a silt. The saturation distribution of NAPL and water were determined using gamma ray attenuation techniques. Mixing soils of contrasted texture, separation of the fine particles in the air when pouring the soil and bulging of the two-dimensional flume during saturation lead to a visibly non-homogeneous sample. Despite the heterogeneities the pollutant plume was perfectly symmetrical. This was attributed to the small scale of the heterogeneities and to a predominantly gravity driven flow due to the large NAPL spill volume. Due to the high retention capacity of the fine soil, no sharp drainage front was observed. It was recognised that the accuracy of the gamma system was arguable when measuring dynamic saturation profiles and it was also highly dependent on the initial conditions.

DNAPL experiments in saturated inclined layered sand

The aim of the DNAPL experiments was to observe the effect of an inclined coarse sand layer imbedded between two finer sand layers on the movement of a DNAPL spill. This work was motivated by the research done by Poulsen and Kueper (1992). From a field experiment of a small DNAPL spill, they found that the DNAPL would reach different depths depending on whether the release is instantaneous or a slow drip release. It was suggested that the depth of penetration from any release could be plotted against the volume of the release. However, the number of data points in the plot is very few and covers only volumes of the order of 5 to 10 litres and depths of the order of 10 to 20m. The plot extrapolates the available data and cannot be considered reliable. Another issue that rises from their work is the effect of soil layer inclination on the migration of the DNAPL. The field experiment by Poulsen and Kueper was conducted in sands which showed distinctive soil layering with an inclination of 5 degrees. The angle of inclined soil layer will affect the migration of DNAPL in the soils.

The experiments conducted at Boulder aimed at answering the following questions:

- how long will it take for a DNAPL spilled on the top to penetrate the inclined layer and eventually reach the bottom of the tank?,
- how far horizontally, from the injection point, will the DNAPL travel before it will start penetrating the coarse layer and likewise the horizontal distance within the coarse layer and in the end the total horizontal distance it has travelled within the tank?, and
- how deep in the sand will the DNAPL travel?

EXPERIMENTAL STUDY OF LNAPL MIGRATION IN A LOAMY SAND

1 Experimental set up

1.1 Two-dimensional tank

The LNAPL spill experiment was conducted in a two-dimensional tank which was 180 cm high, 120 cm long and 5cm wide. The tank consisted of two Plexiglas walls 1.9cm thick and the front Plexiglas wall was lined with 0.63 cm tempered glass on the inside. The walls were bolted to a rigid steel frame, which was in turn bolted to steel end plates. Two horizontal steel supports were bolted to the steel frame at the back of the tank to reduce deformation whereas one only was bolted to the steel frame at the front of the tank to allow better visual monitoring of the contaminant migration during the experiment (Plate-1.a).

1.2 Porous media

One uniform fine silica sand obtained from crushed sandstone (UNIMIN Corp.) with a Taylor mesh size #70 was mixed manually with a natural silt extracted from a sedimentary formation at the Bonny Dam site, eastern Colorado. The mixture consisted of 15% Bonny Silt and 85% #70 Sand (mass ratio). This resulted in a soil with 16% of silt-sized particles (<63 μm), which correspond to a Loamy Sand textural class (UK classification). Soils characteristics are given in Table-1.

Table-1: Characteristics of Sand #70 and Bonny Silt

Soil type	Hydraulic conductivity ($m.s^{-1}$)	Intrinsic permeability (m^2)	Specific gravity ($g.cm^{-3}$)	Dry bulk density ($g.cm^{-3}$)	Mean grain size (mm)	Uniformity coefficient
Bonny silt	$1.0\ 10^{-6}$	$1.02\ 10^{-13}$	2.63	1.55	-	-
Sand #70	$2.44\ 10^{-3}$*	$2.78\ 10^{-11}$*	2.64+	1.60*	0.198*	1.86*

* Illangasekare et al., 1995

+ Armbruster, 1990

1.3 Test fluid

The lighter than water Non Aqueous Phase Liquid used was Soltrol 220 (Phillips Petroleum Inc.). Soltrol 220 is an Isoparaffinic solvent which is a mixture of C_{13} to C_{17} hydrocarbons chains that has negligible solubility in water. The fluid properties are summarised in Table-2. Soltrol 220 has low toxicity by dermal contact and inhalation. It is colourless and was dyed red with Sudan Red IV (insoluble in water) to enhance visual observations. Soltrol 220 has a mass attenuation coefficient similar to water and it was mixed with 1-Iodoheptane to increase the liquid attenuation coefficient for gamma radiation. A volume ratio of 1 to 9 of Iodoheptane to Soltrol was used according to Lenhard and Parker (1987).

Table-2: Fluid properties

Fluid	Density ($g.cm^{-3}$)	Dynamic Viscosity (cP)	Surface tension with water ($Dynes.cm^{-1}$)	Surface tension with air ($Dynes.cm^{-1}$)	Vapour pressure (psi)
Water	0.998*	1.0*	-	72*	-
Soltrol 220	0.789+	4.82+	42+	27+	0.004+
Soltrol 220 + Iodoheptane	0.850+	3.79+	-	-	-

* Host-Madsen, 1989

+ Walser, 1995

1.4 Soil mixing and packing

The silt was crushed and sieved with a 425 μm mesh size to eliminate coarse aggregates of silt particles. The sieved silts were then mixed manually with the sand using a mass ratio of 15 to 85 of silt to sand. Manual mixing of the two soils visibly did not provide a homogeneous mixture, but mechanical mixing in a clay mixer was too fast to prevent the finer particles from separating in the air and this method was discarded. Additionally the silt should have been sieved with a finer mesh size since a large amount of coarse aggregates were still found to be present in the soil after mixing.

The amount of silt increases the proportion of smaller pores and the water retention capacity of the soil; therefore the height of the capillary fringe above the water table increases. With such soils the height of the unsaturated zone is limited by the size of the

tank. As contaminant lighter than water spreads on top of the capillary fringe, the depth of the unsaturated zone has to be deep enough for an LNAPL spill to be of any interest. Preliminary characterisation of water retention curves for mixtures with different proportions of similar silt and sand were performed. The results showed that a mass ratio close to 20 to 80 of silt to sand would allow an unsaturated zone deep enough in the 1.8m high tank to perform a LNAPL spill (providing that the water table is maintained at a low depth).

Before packing the tank with the mixed soil, a 5cm thick gravel layer was deposited at the bottom of the tank to allow uniform water drainage. The tank was dried pack using the drop sieve method in which the soil is deposited in layers through a PVC tube, 3cm in diameter, fitted with a wire mesh sieve. A fine mesh would result in the fines to separate and, therefore, a coarse mesh was used. Since the velocity of soil particles flow through the tube was large, the soil had to be dropped from a small height (2cm) at a fast lateral speed. Layers of 5 to 10cm were deposited in sequence and compacted by tamping. As resistivity probes were inserted at the back of the tank for additional water content measurements, the soil had to be poured close to the front wall of the tank. This resulted in the soil to fill up the tank faster near the front wall allowing the coarse sand particles and silt aggregates to roll down filling the gap at the back of the tank. This created a more heterogeneous layered system at locations close to the back wall of the tank than the front (Plate-1.b).

1.5 Saturation procedure

After the packing, the tank was flushed with CO_2 from the bottom at a small flow rate for 24h. CO_2, which is denser than air, was used to displace air in the tank before saturation because of its higher solubility in water. The tank was then saturated by capillary rise from the bottom with distilled water using a constant head tank (Plate-1.a). The constant head tank was raised step by step until the water table reached the soil surface. The flume was left undisturbed overnight to allow any entrapped CO_2 to dissolve into the water. The constant head tank was then lowered gradually to create unsaturated conditions. The water table level was set up 15cm above the base of the flume. Because of no sharp decrease in water content above the capillary fringe for finer soils, the height of the capillary fringe was not visible.

As the tank was saturated with water and the total horizontal stress increased, the tank expanded in a non-uniform manner because of bulging of the Plexiglas walls. This gradual increase in volume, especially in the middle of the tank, resulted in the soil to sink at some point in the upper part of the tank. Plate-1.c shows a silty layer at the back of the tank, which has settled by approximately 10cm, and the corresponding shear planes due to soil failure. When the water table was lowered and the water drained out of the tank the bulging tended to decrease. To further decrease the lateral movement, wooden wedges were subsequently placed between the tank walls and the horizontal steel supports. Bulging was then estimated by measuring the distance between the walls and a horizontal string attached to the steel frame. It was calculated that the internal thickness of the tank would vary from 5cm to almost 8cm. The attenuation of gamma radiation used to measure the saturation is sensitive to the path length of the radiation and hence to the thickness of the tank. To take into account the increase in the path length during saturation calculation, the internal thickness was measured at every node on a 10cm square grid. It was assumed that the NAPL spill (small volume) would not increase the path length further.

1.6 Saturation measurement using dual-gamma spectroscopy

Gamma photon densitometry is a commonly used method for measurements of soil densities and fluid saturations in porous media. Both single and dual source or energy gamma system have been used extensively in the past(e.g. Reible et al., 1990, Madsen and Jensen, 1991, Lenhard and Parker, 1992, Illangasekare et al., 1995). This technique is based on the principle of unique levels of energy absorption by different materials. The University of Colorado gamma system uses two collinear radioactive sources: Americium 241 and Cesium 137. The energy peaks of the sources are at 60 keV for ^{241}Am and 662 keV for ^{137}Cs with respective half life of 30 and 458 years. The source materials and the detection equipment are mounted to a gantry system, which allows horizontal and vertical movement as shown in Plate-1.d. The source are located near the back wall of the flume and the NaI scintillation photomultiplier tube placed on the front side detects the intensity of the gamma rays after they have penetrated through the flume and its components. The resulting energy spectrum is processed on a microcomputer based multi-channel analyser (ORTEC 918A ADCAM). Detailed specification of the design of the gamma isotopes container, hardware and software used at the University of Colorado, at Boulder, can be found in Armbruster et al.,1990

and Compos, 1997.

The factors that affect the accuracy of gamma measurements include:

- counting time
- sample path length
- variations in the sample porosity
- source intensity
- attenuation coefficient of the pollutant
- detection equipment
- source-detection geometry
- gamma beam diameter

Use of gamma spectroscopy for the measurement of bulk densities and fluid content in porous media is based on the exponential law for monoenergetic gamma radiation. This is a modified form of Lambert's law for light transmission through an absorbing medium. This yields to the Beer-Lambert law which describes the attenuation of monoenergetic gamma rays throught a system with n components:

$$I = I_o \exp\left[-\sum_{i=1}^{n} \mu_i \rho_i x_i\right] \qquad \text{eq.1}$$

where:

I_o: incident count rate

I: emergent count rate

μ_i: mass attenuation coefficient for the phase i (cm^3/g)

ρ_i: density of the phase i (g/cm^3)

x_i: path length through the phase i (cm)

In gamma spectroscopy the rate of energy transmission is described in terms of counts per unit of elapsed time. A count refers to a recorded gamma emission. The count rate will decrease if attenuating materials are placed between the radiation source and the detection equipment. If the effective absorption rate of a material is known, it is possible to predict the mass or the volume of the material by comparing the detected count rate

measured with and without the absorbing material being present.

- For a four-phase system (soil-air-water-LNAPL: LNAPL experiment) eq.1 takes the form:

$$I=I_c\exp\{-(\mu_s\rho_s(1-n) + \mu_w\rho_w S_w n + \mu_o\rho_o S_o n)x\} \qquad \text{eq.2}$$

where the subscripts s, w and o stand for solid, water and NAPL, I is the attenuated gamma intensity, I_c is the initial gamma intensity through the empty tank, S_i is the saturation of phase i and x is the travel distance or the path length of the gamma ray through the phase i with $x_i = nS_ix$. In this equation the attenuation due to air represented by the term $\mu_a\rho_a S_a n$ is neglected because of its low density compared to the other phases.

Eq.2 can be simplified and written for both sources by using the dry bulk density $\rho_b=\rho_s(1-n)$, the volumetric fluid content $\theta_i = S_in$ and by writing $U_i = \mu_i\rho_i$, noting that the attenuation due to the soil is constant: $I_d = I_c \exp-[\mu_s\rho_b x]$

$$I_{Cs} = I_{Csd}\exp\{-[U_{Csw}\theta_w + U_{Cso}\theta_o]x\}$$
$$I_{Am} = I_{Amd}\exp\{-[U_{Amw}\theta_w + U_{Amo}\theta_o]x\} \qquad \text{eq.3a-eq.3b}$$

If the initial count rates through the tank filled with dry soil (I_{Csd} and I_{Amd}) are measured and the lumped attenuation coefficients for water and NAPL (U_{Csw}, U_{Amw}, U_{Cso}, U_{Amo}) and the path length x are known, eq.3 can be solved simultaneously for the water and the NAPL volumetric content.

This method assumes that the dry bulk density and the path length are constant throughout the experiment. As noted earlier, due to the internal pressure exerted on the tank walls, the tank expanded when the soil was saturated. In addition some settling of the soil also occured which increased the density. Another method is to measure the initial count rate I_c for both sources through the empty tank and the count rate thought the soil saturated with water, noting that at full saturation $\theta_w=nS_w=n$, eq.1 becomes $I=I_c\exp\{-(\mu_s\rho_b + U_w n)x\}$, and when written for both sources it can be solved

simultaneously for the dry bulk density and the path length. With this method, the attenuation coefficient due to the soil μ_s must be measured a priori. This method does not take into account the probable reduction in path length during de-saturation as the load on the walls of the tank is decreasing.

It was decided to assume the dry bulk density to be constant but to measure the path length manually (as described above) in order to use the first method of calculation.

- For a three-phase (soil-water-DNAPL: DNAPL experiments) eq.1 takes the same form as eq.2 because the air phase attenuation has been neglected in the four phase system.

If $I_o=I_c\exp\{-\mu_s\rho_s(1-n)x\}$ is the initial count rate measured through the dry soil, the count rate through the fully saturated soil with water (i.e $S_w=1$) can be written:

$$I_d=I_o\exp\{-(\mu_w\rho_w n)x\} \qquad \text{eq.4}$$

measuring I_d through the fully saturated soil and knowing μ_w, eq.4 can be solved for n assuming that the path length x is known and equal to the internal thickness of the tank. It should be noted that in the DNAPL experiments, bulging did not seem to occur due to the small size of the tank and the reduced load onto its walls.

When DNAPL is introduced into the system the count rate through the tank containing three phases is written:

$$I=I_o\exp\{-(\mu_o\rho_o S_o n + \mu_w\rho_w S_w n)x\}$$

$$\Leftrightarrow \quad I=I_o\exp\{-(\mu_o\rho_o S_o n + \mu_w\rho_w(1-S_o)n)x\} \qquad \text{with by definition } S_w=1-S_o$$

$$\Leftrightarrow \quad I=I_o\exp\{-(\mu_o\rho_o S_o n + \mu_w\rho_w n-\mu_w\rho_w S_o n)x\}$$

and using eq.4

$$I=I_d\exp\{-(\mu_o\rho_o-\mu_w\rho_w)S_o nx\} \qquad \text{eq.5}$$

knowing μ_o and μ_w, eq.5 is solved for S_o:

$S_o=\ln(I_d/I)/ (\mu_o\rho_o-\mu_w\rho_w)nx$ eq.6

As explained above, in this experiment, the knowledge of the attenuation coefficients of water and Soltrol 220 (+ Iodoheptane) for both sources were needed (eq.3). The lumped attenuation coefficient $U_i= \mu_i\rho_i$ (cm^{-1}) were determined using eq.1 and solving for U_i. To do so, total counts for each fluid and both sources were recorded through a multi-chambered Plexiglas box. Each compartment had an internal thickness of 2.5cm. The effective path length traversed by the gamma energy beam can be increased by sequentially filling the compartments of the box with the fluid of interest. If I_o is the initial count rate through the empty container and I the count rate through a given number of filled compartment (i.e. a given path length); then when $\ln(I_o/I)$ is plotted against the path length a straight line results. The slope of the linear regression is equal to the attenuation coefficient (Figure-1.a-1.b).

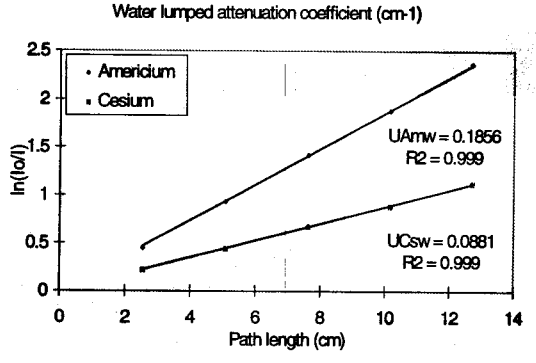

Figure-1.a:Water attenuation coefficient

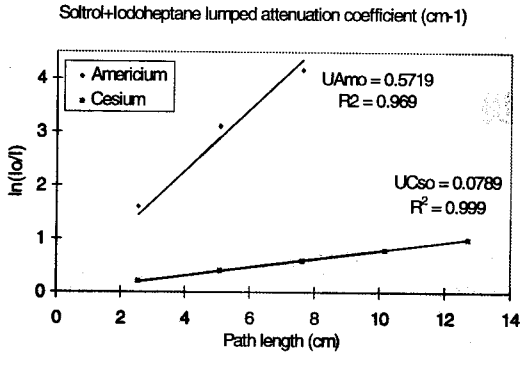

Figure-1.b:NAPL attenuation coefficient

2 *Result of the experiment and discussion*

2.1 Initial saturation and de-saturation

The flume was packed, saturated and de-saturated as described in section 1.4 and 1.5. A 10cm square grid was drawn on the front wall of the tank and used to monitor gamma scanning locations as well as the contaminant migration. In the following x will refer to the horizontal axis with its origin at the bottom left corner of the tank and y to the elevation above the base of the tank. The soil surface was located at y=170cm.

Figure-2 shows the water content varying with elevation measured at different horizontal locations before the spill.

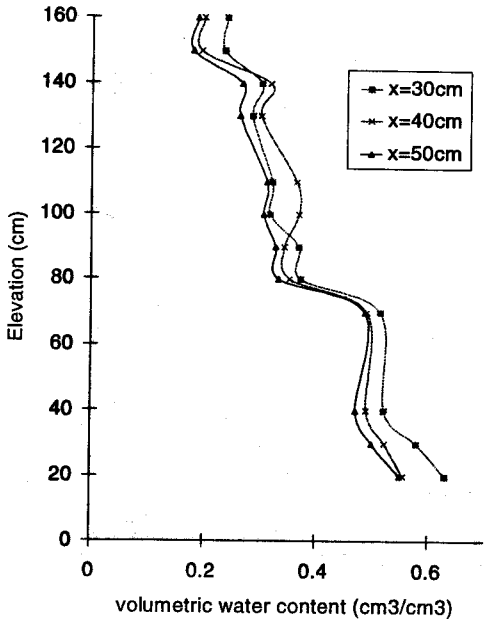

Figure-2: Water content profile

The slight apparent decrease in water content from y = 20 and 40cm is likely to correspond to an increase in bulk density at the bottom of the tank. This would increase the attenuation capacity of the four phase system and would be considered by the gamma measurement as an increase in water content. The decrease in water content occurring around y = 70cm corresponds to the air entry point of the soil and therefore to the top of the capillary fringe. It was not possible to visibly distinguish a saturated region from an unsaturated region as no change in colour due to saturation variations occurred in the soil. The overall relatively smooth variation in water content through the profile is expected with soils with finer texture. Above y = 80cm the water content decreases slightly towards residual water content. The sudden further decrease in water content from 140cm up to the soil surface may be due to a reduction in bulk density, knowing that some extra soil had to be added after the soil failure occurred (as described in Section 1.5). Another possibility is that evaporation is occurring at the soil surface. To prove these hypotheses, further measurement of the static water retention curve would be needed. Knowledge of the water characteristic curve would also confirm if the static equilibrium has been reached or not. The tank was left to drain for

only 24h; thus, it is probable that static distribution was not achieved even though no significant volume of draining water was observed at the drainage outlet.

2.2 LNAPL migration

A total volume of 3.5l of Soltrol 220 mixed with Iodoheptane was injected under a constant head of 10cm. The constant head injection source (described in the DNAPL experiments) was placed at x = 40cm and 5cm below the soil surface. Digital pictures of the pollutant plume (Plate-2 and Plate-3) were taken from a fixed distance at different time intervals, while vertical gamma scanning (x=40cm) was performed mostly overnight following the advancing front under the injection source.

Plate-1.e shows the contour lines of the Soltrol migration. The contaminant infiltration front has travelled approximately 80cm in 70 hours where its advancing velocity became too small to be monitored. The vertical velocity of the advancing front was almost constant in the first 10cm at about 120mm/s. After 70 hours it reduced gradually down to velocities lower than 0.012 mm/s. This reduction in velocity corresponds to a decrease in relative permeability of the NAPL as water contents increases towards the capillary fringe. As expected, these infiltration velocities are much smaller than velocities observed in coarser sands. Illangasekare et al., 1995 report similar experimental set up with smaller spill volumes (0.5l) of DBP in a #30 sand where the contaminant travelled approximately 60cm in 3 hours.

The spreading of the Soltrol plume with time is shown in Plate-2 and Plate-3. A major observation is that the plume is perfectly symmetrical vertically despite the observed micro-heterogeneities created during soil pouring (i.e. thin silty layers). Since the randomly spaced silty layers have high retention capacity of water, it was expected that they would act as capillary barriers, increasing the lateral spreading of the contaminant and lead to an irregular plume shape. The scale of the heterogeneities may be two small to affect the overall shape of the LNAPL plume, but, as suggested by the gamma radiation measurements, it is probable that higher volumes of NAPL are being retained in the silty layers. Hjeldnes et al (1995) showed that the ratio of the plume width to the plume depth increases with decreasing water content. They also observed that if a spill occurs in dry conditions (i.e.two-phase air-NAPL), larger lateral spreading occurs and

the shape of the plume is less regular and symmetrical. This is due to high capillary forces between NAPL and air taking place in smaller pores in dry conditions with NAPL acting as the wetting fluid. In the present case, the water contents were high because of the high retention capacity of the soil. NAPL flows preferentially through larger pores, displacing air, while smaller pores are occupied by water. Also, capillary forces between NAPL and water are small compared to that of NAPL and air. In the lower part of the tank where water content increases, the size of the plume is growing vertically. In the upper part of the tank, below the injection source, the NAPL is spreading both horizontally and vertically at the same rate giving a circular plume.

A second spill was initiated in order to observe the Soltrol to spread on top of the capillary fringe. This time the NAPL was dyed with Automate Red dye(Morton Int.) giving it a bright burgundy colour. Plate-1.f shows the LNAPL spreading onto the top of the capillary fringe at around y = 40cm. Comparing to the initial water content profile measurement shown in Figure-2, the capillary fringe was depressed by approximately 30cm.

The water and total fluid content profiles varying with time are shown in Figure-3. The profiles show some small peaks of fluid contents (e.g. at 135 and 145cm) suggesting non homogeneous distribution of the fluids. These variations in fluid contents throughout the profile, occurring at almost every 5-10cm, could be interpreted as discontinuities due to soil layering (the tank was filled by pouring layers of 5-10cm).

The general trend of the dynamic profiles is typical of a three immiscible fluid system (e.g. Eckberg and Sunada, 1984). The advancing NAPL front is visible (Figure3-a.b.c.d.e.f.g.h). The amount of NAPL being retained is high and almost constant through the profile but a drainage front is visible in the top 15-20cm when NAPL redistribution starts and all the spill volume has been injected (Figure3-i.j.k.l.). The water content is almost constant with time in the upper part of the tank (100-160cm) suggesting residual water conditions whereas at the NAPL front, toward the capillary fringe (60-90cm), water content is decreasing as water is being displaced by NAPL.

Figure-4 shows the NAPL distribution profile varying with time. Figure-4.a shows

clearly the infiltrating NAPL front in the earlier times with drainage taking place in the upper part. However a sharp draining front is not visible even after long periods of time and the amount of NAPL remaining in the upper part of the profile is relatively high (Figure-4.b). This is explained by the high retention capacity of the silty soil and the low relative permeability of the NAPL due to high water contents throughout the profile.

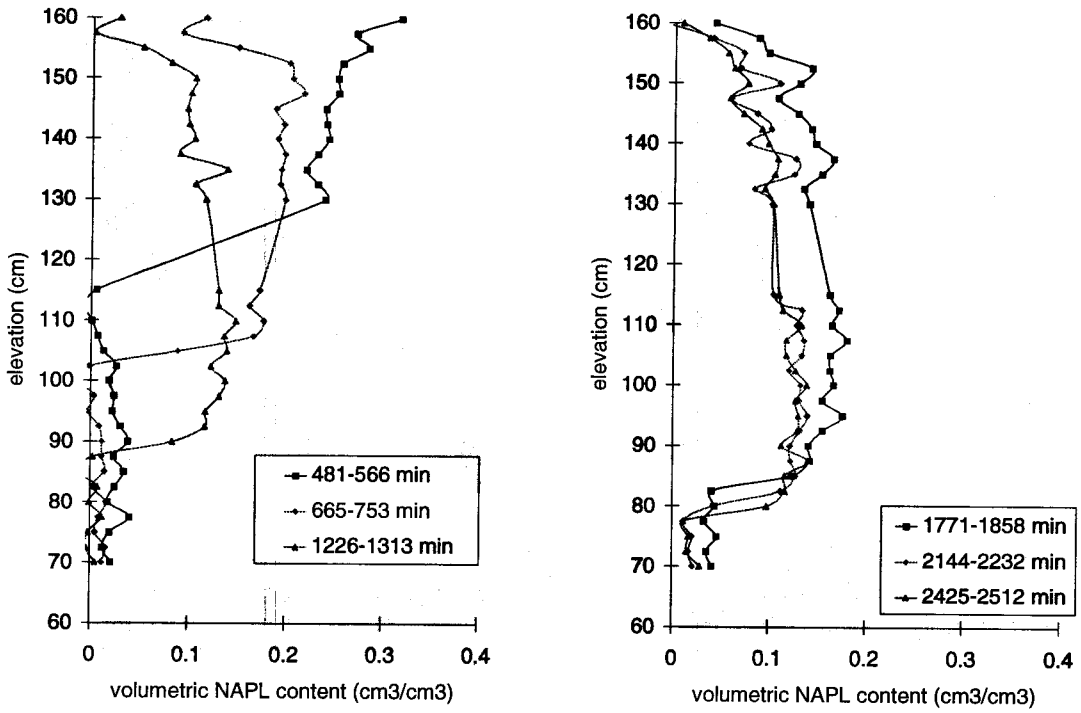

Figure-4:NAPL profile varying with time

3 *Final remarks*

- Mixing two soils of contrasting textures proved to be very difficult. When mixture of sands and fines is poured in the tank, fines tend to separate easily in the air creating a non homogeneous sample. It is recommended to use soils with no gap in their grading and they should be mixed mechanically.
- When using the sieve drop method to pack the tank, care should be made to select the optimal mesh size of the sieve in order to avoid separation of the fine soil particles.

The height at which the soil has to be dropped should be minimal and the lateral speed at which it is dropped should be high.

- In a large two-dimensional tank, bulging of the Plexiglas walls occurs when the soil is saturated with water. This bulging leads to soil settlement and to a loss in contact between the soil and the tank wall at certain locations. In addition, the bulging increases the gamma radiation path length and leads to overestimation of fluid contents by the gamma system. Reinforcement should be used to support the Plexiglas walls and/or they should be lined with glass.
- Use of gamma radiation to measured fluid contents has proved efficient in many past contaminant migration studies. The major drawback of the method is its inadequacy to capture dynamic processes. In fact, at a given location, the fluid content is averaged over the length of time for which the scanning lasts and therefore changes in fluid content during this time can not be monitored. Hence, the representation of a fluid saturation profile is only valid when the rate of moving fluids is very slow. For each data set presented in Figures 3 and 4, there was a gap of 1h30min between the first and last measurements. For more accurate results, the scanning time at each location should be at least 2min (Walser, 1995).
- The results from dry scanning with the gamma system were used as the reference count rate for water and NAPL content calculation. However, as the soil was saturated and de-saturated, the path length of the gamma radiation through the soil varied due to bulging. At the same time the bulk density increased at some location due to soil settlement. If was found that the bulk densities estimated from the scanning results of the dry soil were not consistent with those estimated from the results of the saturated soils. Since the hypothesis of constant bulk density is not valid, one may consider that the calculation of volumetric fluid content is affected by a systematic error and that the results should be examined as qualitative values only. In addition, errors associated with path length measurement, detector performance and counting rate due to radioactive decay suggest that the interpretation of the results obtained with the gamma system should be done with care.

Figure-3: Water and total fluid content profiles

a) 481-566 min

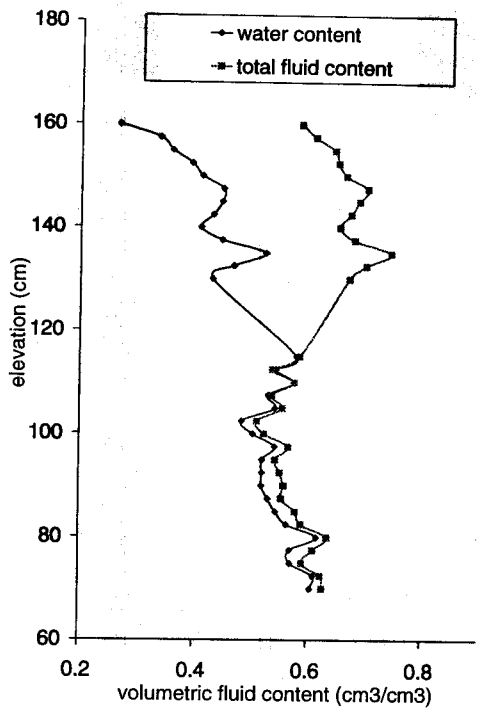

c) 945-1033 min

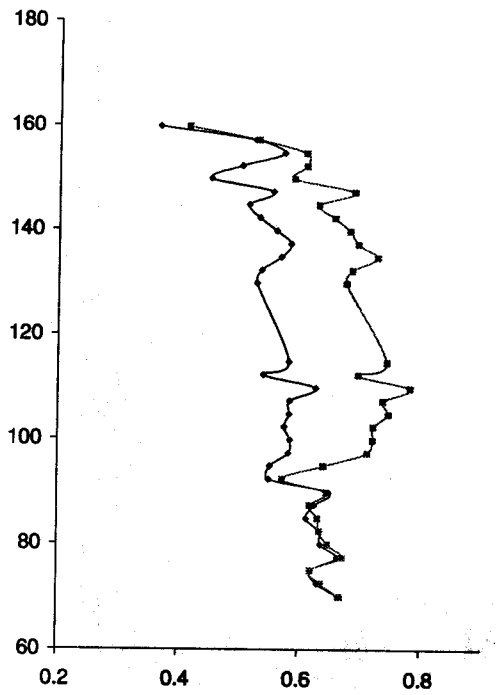

b) 665-753 min

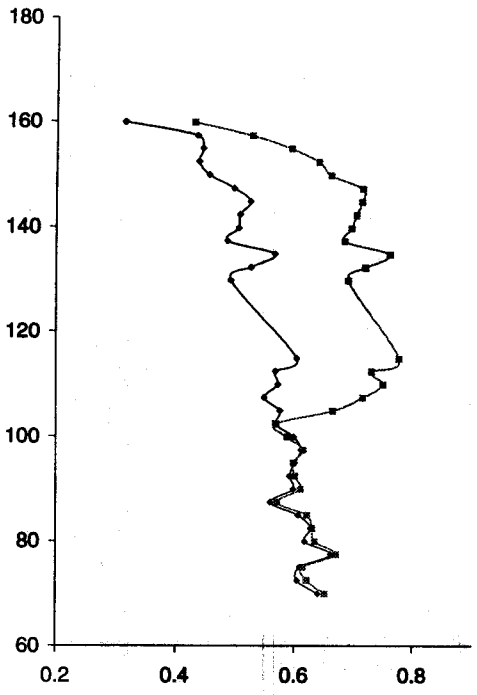

d) 1226-1313 min

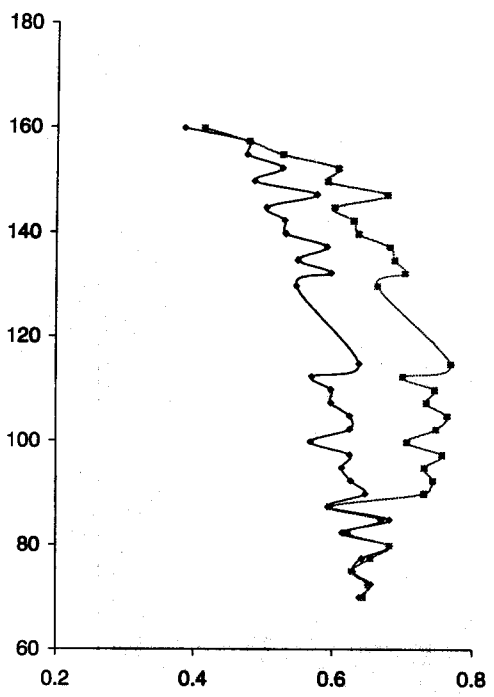

e) 1771-1858 min

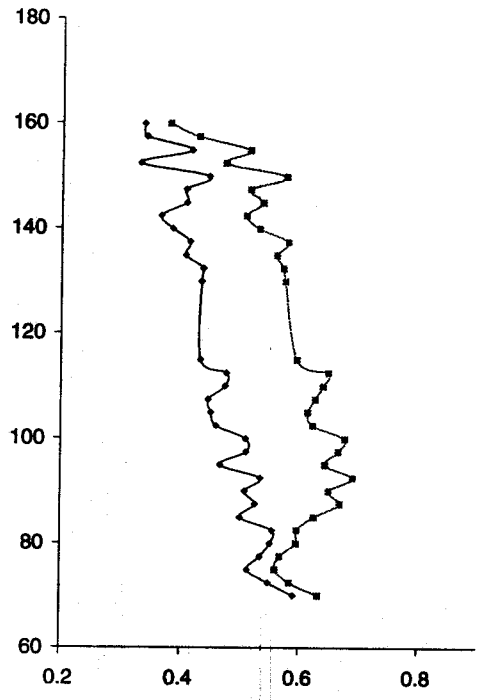

g) 2144-2232 min

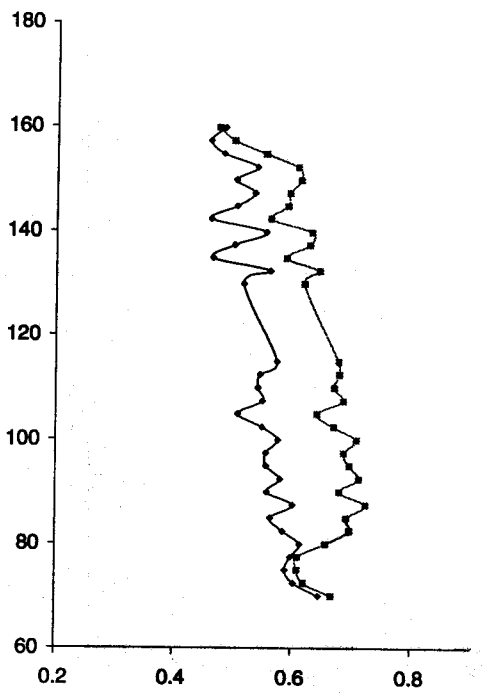

f) 1958-2045 min

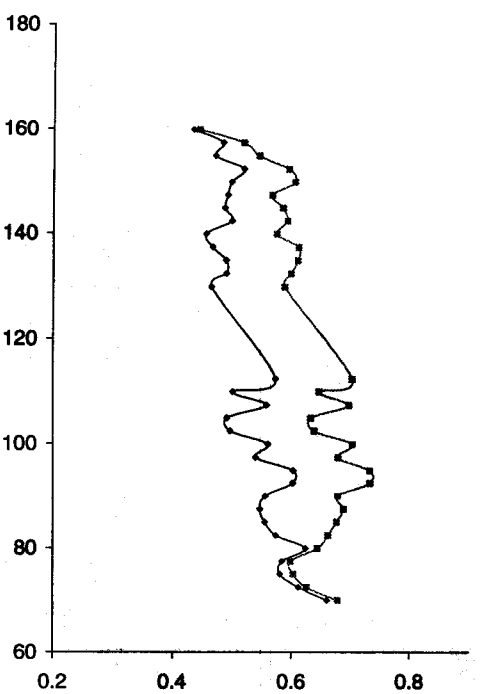

h) 2425-2512 min

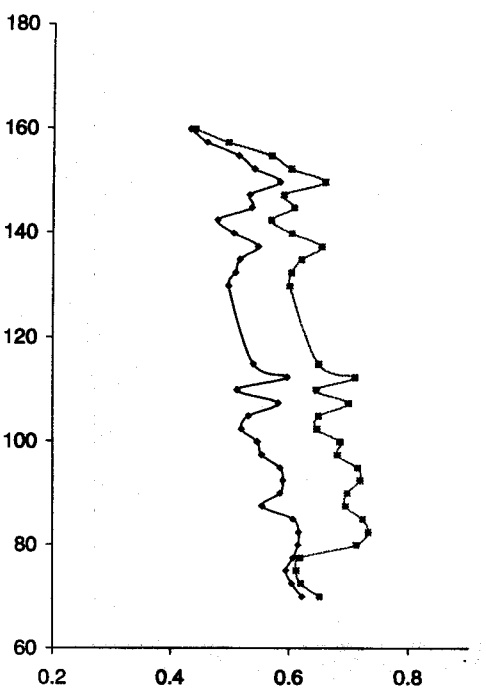

i) 3543-3634 min

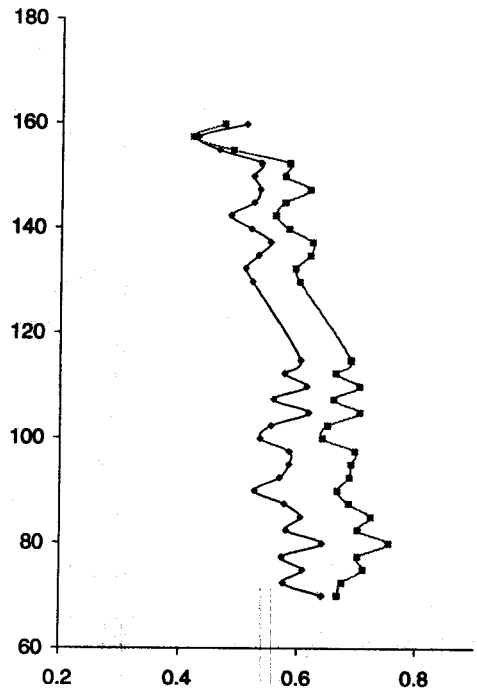

k) 3918-4005 min

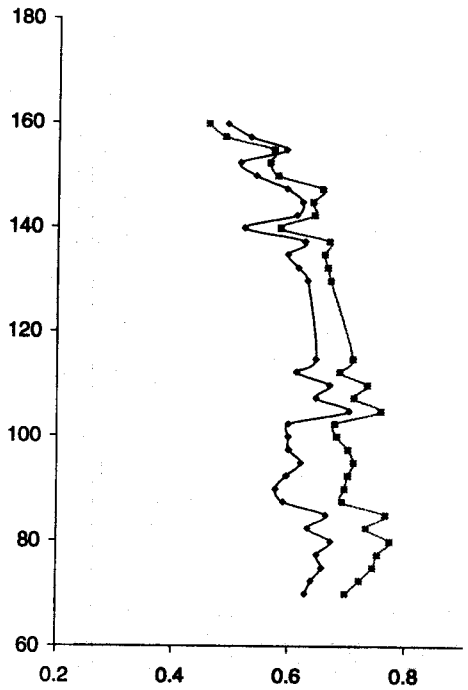

j) 3732-3819 min

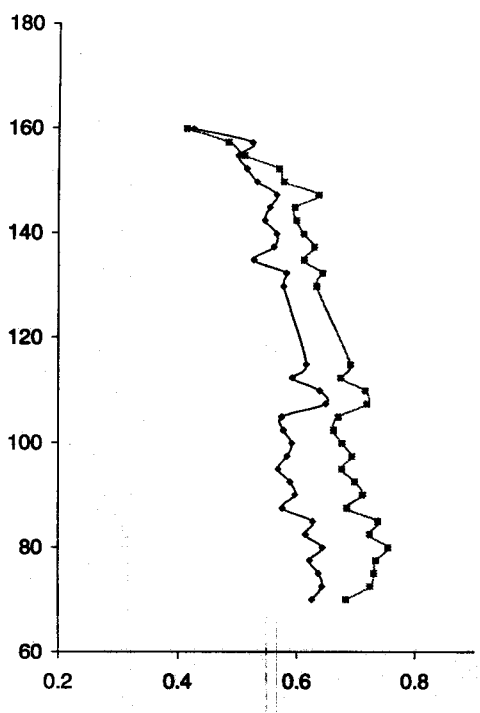

l) 4104-4191 min

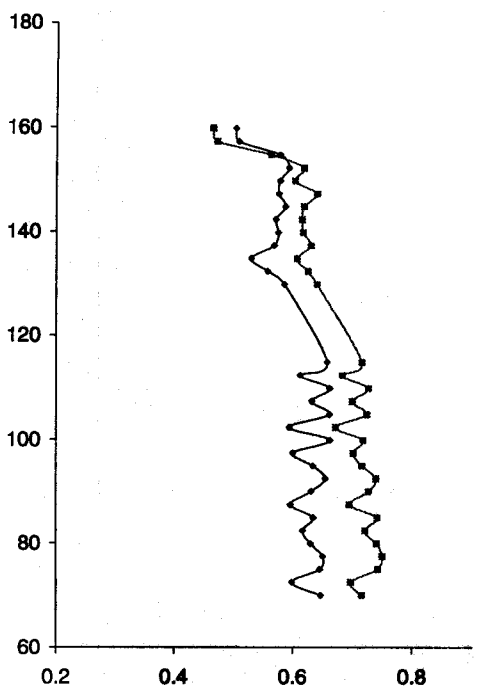

Plate-1:

a)

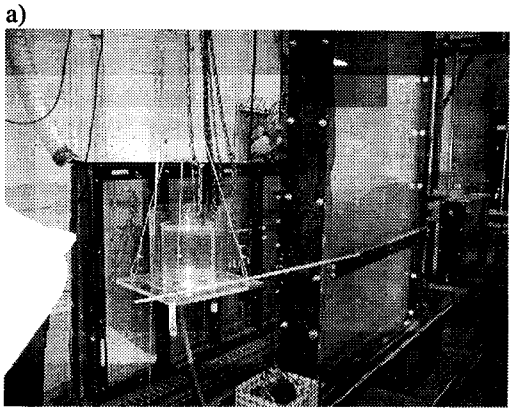

d)

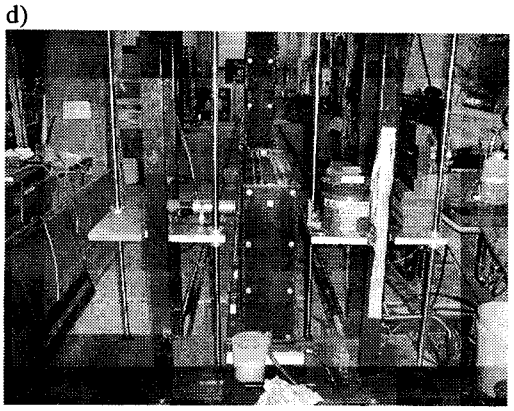

b)

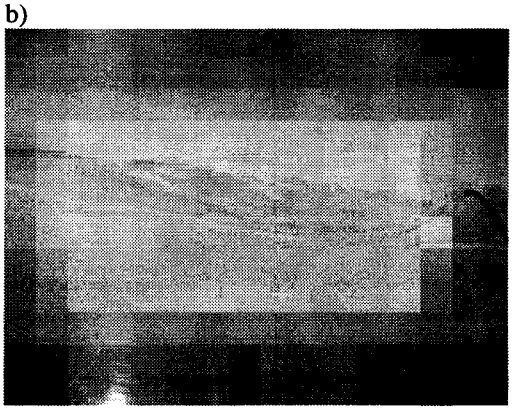

e)

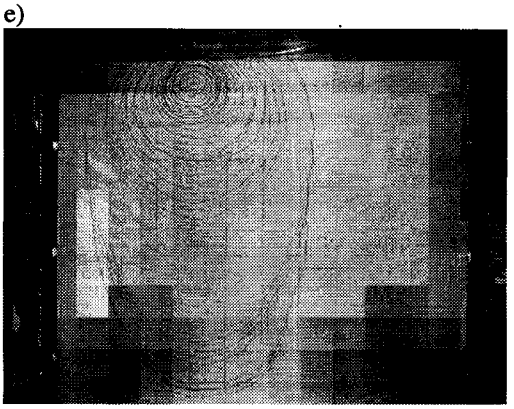

c)

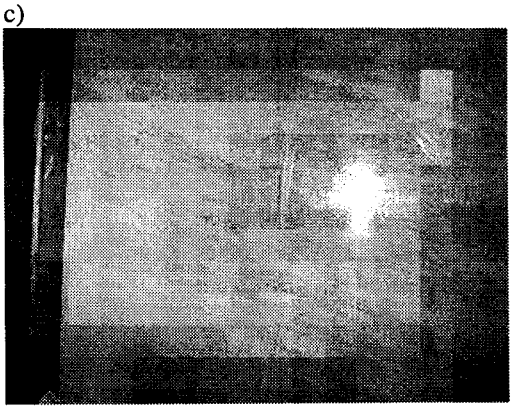

f)

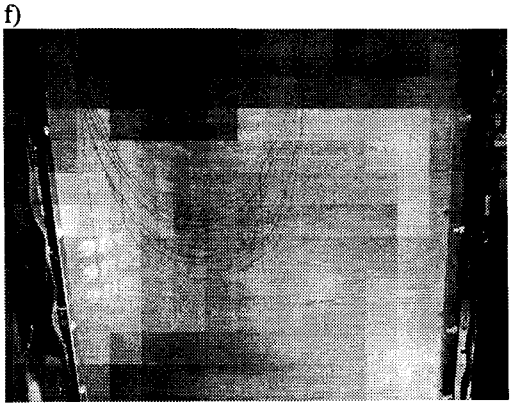

Plate-2:

a) 10 min

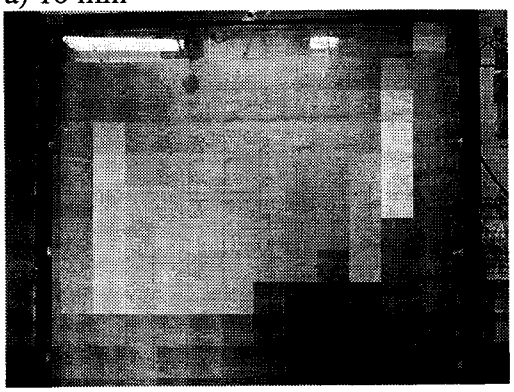

e) 43 min

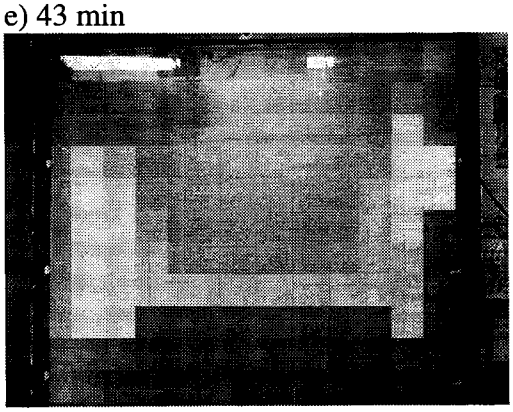

b) 15 min

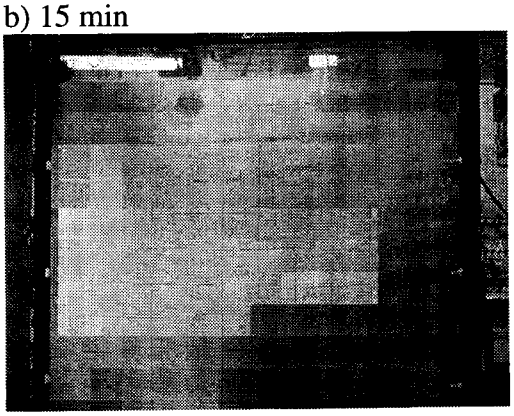

f) 61 min

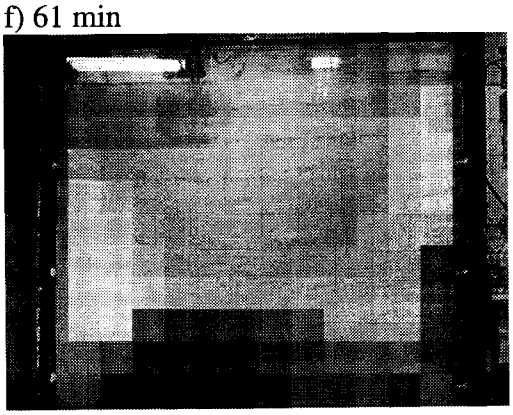

c) 19 min

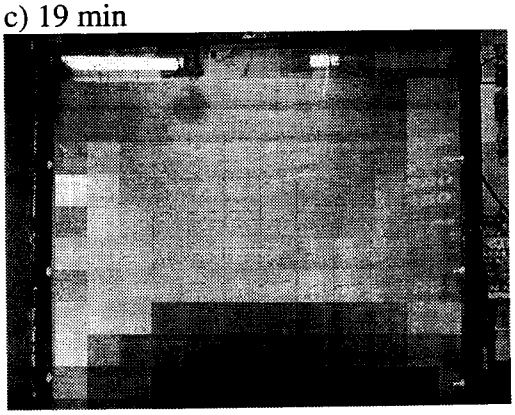

g) 74 min

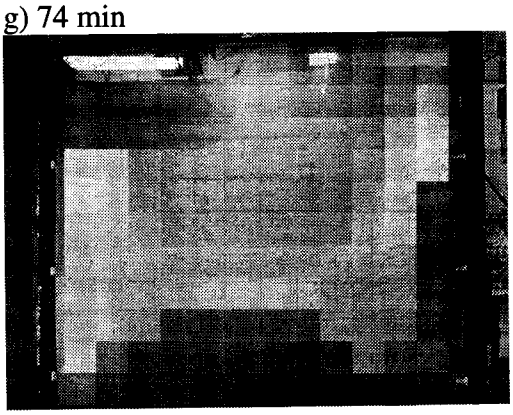

d) 28 min

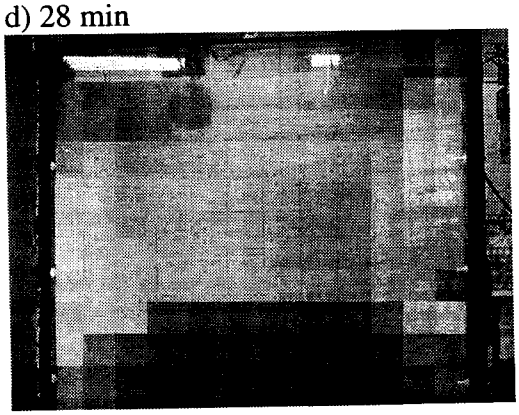

h) 95 min

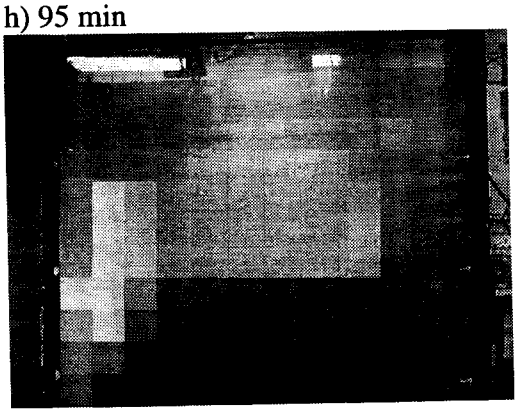

Plate-3:

a) 160 min

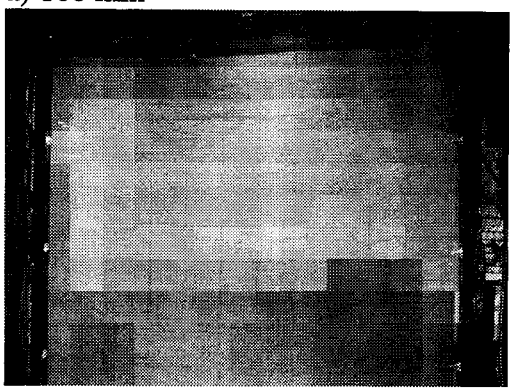

b) 249 min

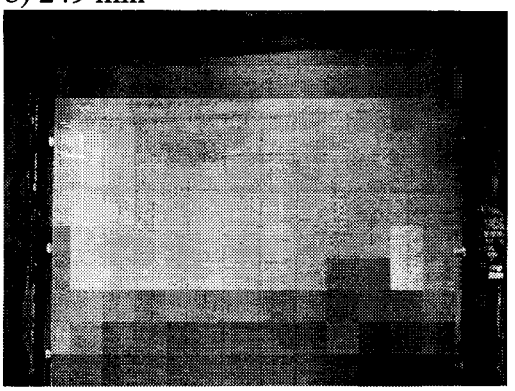

c) 308 min

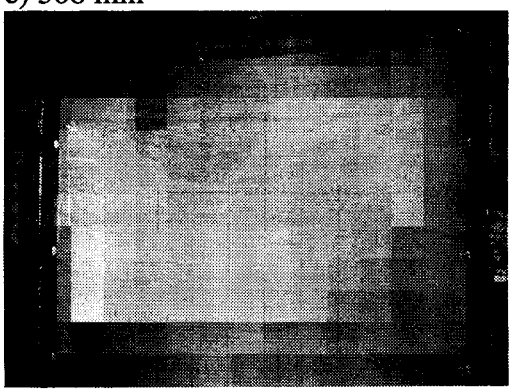

d) 467 min

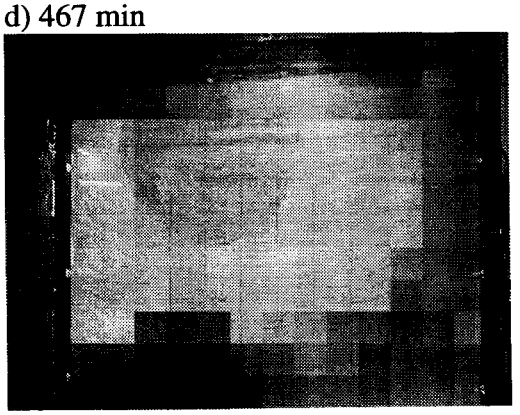

e) 1395 min

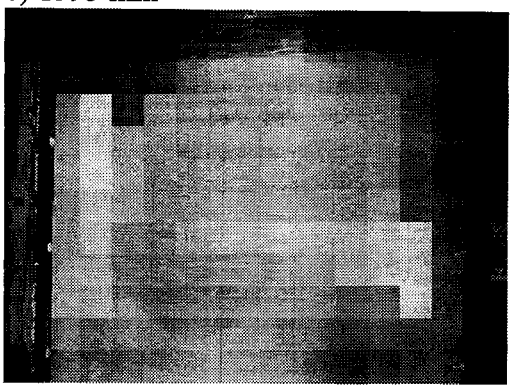

f) 1710 min

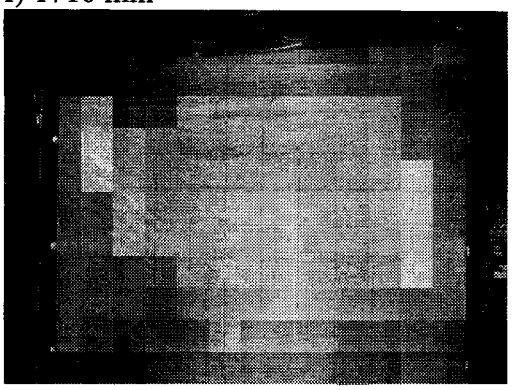

g) 2725 min

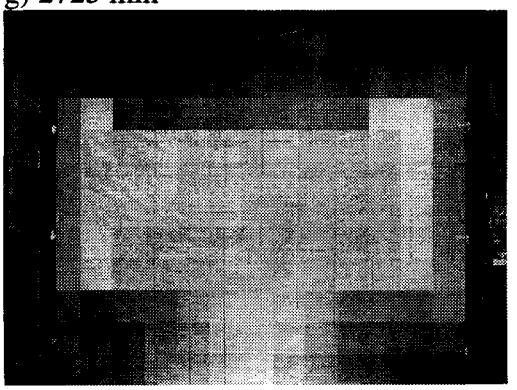

h) 3148 min

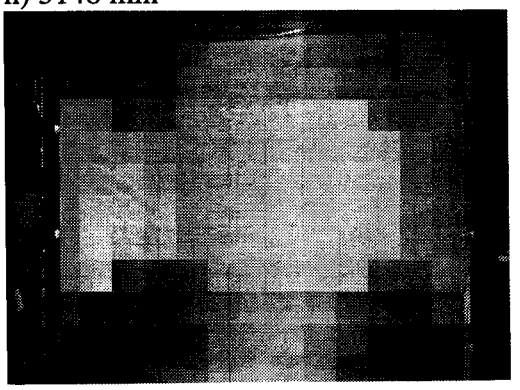

References

Armbruster E.J. (1990). Study of transport and distribution of lighter than water organic contaminants in groundwater. Master thesis. Department of Civil, Environmental and Architectural Engineering, University of Colorado.

Compos R. (1997), Multiphase experimental realizations of Dense Non Aqueous Phase Liquid spreading in saturated heterogeneous porous media, MSc Thesis at the University of Colorado.

Eckberg D.K., Sunada D.K. (1984). Nonsteady three-phase immiscible fluid distribution in porous media. Water Resour. Res. 20-12: 1891-1897.

Hjeldnes E.I., Bretvik S.K., Skoglund K.A., Hylen S. (1995). An experimenal study of oil contamination spreading in sand. pp 373-394. Geoenvironment 2000 vol.1, Proceeding of Speciality Conference, New Orleans, Louisiana, Published by ASCE.

Host-Madsen J., (1989). Immiscible multi-phase flow in porous media. PhD thesis, Institute of Hydrodynamics and Hydraulic Engineering, Technical university of Denmark.

Host-Madsen J., Jensen K.H. (1992). Laboratory and numerical investigation of immiscible flow in soil. Journal of Hydrology, 135: 13-52.

Illangasekare T.H., Ramsey J.L., Jensen K.H., Butts M.B. (1995). Experimental study of movement and distribution of dense organic contaminants in heterogeneous aquifers. J. Contam. Hydrol. 20: 1-25.

Lenhard R.J., Johnson T. G., Parker J.C. (1993). Experimental observation of non aqueous-phase liquid subsurface movement. J. Contam. Hydrol. 12: 79-101.

Parker J.C., Lenhard R.J. (1987). A model of hysteretic constitutive relations governing multiphase flow (1.Saturation-pressure relations). Water Resour. Res. 23-12: 2187-2196

Reible D.D., Illangasekare T.H., Doshi D.V., Malheit M.E. (1990). Infiltration of immiscible contaminants in the unsaturated zone. Groundwater. 28-5: 685-692.

Walser G.S. (1995). Vadose zone infiltration, mobilization and retention of Non-Aqueous Phase liquids. PhD thesis, Department of Civil, Environmental and Architectural Engineering, University of Colorado.

DNAPL EXPERIMENTS IN SATURATED INCLINED LAYERED SAND

1 Introduction

The aim of the DNAPL experiments was to observe the effect of an inclined coarse sand layer sandwiched between medium sand layers on the movement of a DNAPL spill. More specifically the experiments aimed at answering the following questions:

- How long will it take for a DNAPL to penetrate into the inclined layer and eventually reach the bottom of the tank?
- How far horizontally, from the injection point, will the DNAPL travel before it starts penetrating into the inclined coarse sand layer and then into the underlain medium sand layer?
- How deep in the sand will the DNAPL travel?

This work is inspired by the results shown in the paper by Poulsen and Kueper (1992). From a field experiment of a small DNAPL spill, they have shown that the DNAPL will reach different depths depending on whether the release is instantaneous or a slow drip release. They suggested that the depth of penetration from any release could be plotted against the volume of the release. However, the data on which this plot is based is few and covers only volumes of the order of 5 to 10 litres and depths of the order of 10 to 20m. The presented graph extrapolates the available data and can in no way be considered reliable.

Another question rising from the paper by Poulsen and Kueper (1992) is what is the influence of the layer inclination to the migration of the DNAPL. The field experiment was conducted on sands showing distinctive soil layering with an inclination of 5 degrees. The angle of inclined soil layer affected the migration of DNAPLs in the soils.

2 Tank

The tank used was the one described by Compos (1997) and is presented in Fig 1. The dimensions of the tank are 90 cm (length) x 60 cm (height) x 5cm (width). The tank is made of Plexiglas sheets bolted on a metal frame. The interior walls of the tank are lined with glass, serving two purposes: (a) to protect the Plexiglas from the plasticising effects of DNAPLs,

and (b) to prevent the creation of extra pathways by the wall, because Plexiglas attracts NAPL on its surface whereas glass attracts water.

3 Soils

3.1 Sand types

The tank was filled with medium-coarse sand (#30) and a 10cm thick inclined layer of coarse sand (#16) was placed in the middle. The coarse sand layer acts as a pathway, or a sink, for the DNAPL, as it proceeded downwards. This layer had an inclination of 7.5° to the horizontal in the first experiment and 5° in the second experiment. The bottom and the two end vertical walls of the tank were lined with a 5cm thick layer of fine sand (#70), in order to protect the gasket from the plasticising effects of the DNAPL. The configuration of the sand layers is shown in Fig 2. A detail of the tank lining can be seen in the photograph in Fig 4.

The permeability data and capillary pressure-saturation curve parameters for the #30, the #16 and the #70 sands, as given by Ramsey (1992), are shown in Table 1. Their grain size distributions are shown in Fig. 3.

3.2 Sand packing and saturation procedure

Fig. 4 shows the packing procedure and a detail of the pouring of the fine sand lining. The tank was "wet packed" with sand in layers of 2cm from the bottom up, using the "drop sieve" method. This method use a tube fitted with a wire mesh sieve to ensure even distribution of the sand grains. To achieve water saturation close to 100%, sand was poured in the water with 5cm drop from the tube. This minimised stratification occurring within the homogeneous regions but did not eliminate it completely. When each 2cm layer was deposited, it was compacted by tamping and then the top surface was scraped to make a levelled surface and reduce stratification caused by tamping.

For the lining of the vertical wall of the tank, plastic partitions were used. During the pouring of the sand, the level of the fine sand behind the partition was kept at approximately the same level as the level in the matrix to avoid sand flowing in either direction.

De-aired water was used in the first experiment, whereas tap water was used in the second

experiment. At the time of the second experiment, the de-airing device and all the available vacuum pumps were out of order. Therefore, the tap water was left to settle for a few hours, so that air formed bubbles and get de-aired to some extent. It is assumed that this procedure left the sand water saturated with a negligible gas phase content.

4 Injection

4.1 Injection device

The NAPL injection devise used in the experiments is shown in Fig 5. It consists of a small tank with external dimensions of 5 x 10 x 10cm (fitting in the tank) connected to a bigger reservoir via a solenoid valve. The head of the fluid in the small tank remains constant throughout the injection period by a floating switch (fluctuation of ±2mm), which gives a signal to the solenoid valve to open or close. The small tank has an orifice with a diameter of 1.5mm, which can be increased, if necessary. This acts as a point source. An attachment for a line source is also available. Its dimensions are 1mm wide by 5cm long, ensuring that it fits in the flume. Schematic diagrams of the orifice for the point source and of the line source attachment to the orifice are presented in Fig 6.

4.2 Injection fluid

The fluid injected in the tank was TCA (trichloroethane), which is used in dry cleaning businesses extensively. Its properties are summarised in Table 2. It is a highly toxic fluid with a strong odour. It was dyed red using the Automate Red dye, a hydrophobic organic soluble dye produced by Morton Thiokol Inc in Chicago. It was decided to use this dye instead of the commonly used Sudan red, since it is safer and gives a darker burgundy colour to the fluid, allowing for better visual inspection.

4.3 Location of injection

The injection devise was placed on the sand surface over column 4 of the tank (see Fig 12). The tip of the injection orifice was located in row 2. Its co-ordinates from the top left corner of the tank are (20,5) cm (see Fig 12). The injection point is at this depth to prevent the DNAPL from escaping along the orifice and pooling on the sand surface. The eccentric location (20cm from the top left corner, as opposed to the centre at 45cm) was selected

because large horizontal migration along the inclined bottom interface of the coarse and medium sands was expected. The orifice was placed centrally along the longitudinal axis of the tank. A DNAPL head of 10 to 15 cm was selected to overcome the NAPL entry pressure of the saturated sand.

4.4 Shape of injection

In most of the previous laboratory investigations at CU, a line source placed vertical to the walls of the 2D tanks was used. This way, the source was considered to be 2 dimensional in the width of the tank and point source on the plane of the 2D tank. However, this may create wall effects and may result in differences between what is seen on the wall of the tank and what is happening inside the tank.

In order to compare past test results obtained at CU with these experiments, the same source configuration was needed, using the line source attachment of Fig 6. However, it was subsequently found that this arrangement was not feasible because its large opening created a very large injection rate. Therefore, the orifice with the point source was used instead.

4.5 Rate of injection

The rate of injection is limited by:

- the head of the fluid in the injection device,
- the orifice opening (in this case the diameter of the orifice opening), and
- the permeability of the sand that the DNAPL encounters first.

The injection device maintained a constant head of fluid of 10cm ±2mm and had an orifice-opening diameter of 0.5mm. This configuration, when filled with water and left to flow in the air, gave a rate of flow of 500ml / (2min, 4s) = 500ml / 160s=3.12×10^{-4}lt/s. However, the rate of the injection of the TCA was smaller in the experiments, because it was constrained by the permeability of the sand.

5 Measuring techniques

During the course of the DNAPL experiments two types of data were collected. One was qualitative by photographs showing the location of the DNAPL plume at different times and the other was quantitative by γ–rays attempting to capture the saturation of the DNAPL at a

specific location and time.

5.1 Qualitative data = digital photographs

While the flow of the DNAPL was still fast (the dynamic phase of the experiment), the DNAPL front was followed on the front and back of the glass walls of the tank by visual inspection. The DNAPL was dyed red in order to make imaging of its location possible. Contours were drawn on the walls of the tank at specified time intervals and also photos were taken using a digital camera.

5.2 Quantitative data = γ-rays scanning

Once the front of the DNAPL stopped moving fast, at about 1h after the end of the injection, the saturation of DNAPL was measured by the γ-rays attenuation system. The γ-rays attenuation system is described in detail in the previous section (LNAPL experiment). The tank along with the γ-system is shown in Fig. 7.

5.3 Measurement of the lumped attenuation coefficient for TCA

A five-chambered acrylic box is normally used to determine the lumped calibration constants of a liquid. Each chamber of the box is 12.5 cm by 12.5 cm and has a width of 2.5 cm. An initial value is obtained through the empty box, then the chambers are successively filled and the count rate of the γ-rays is measured. Linear regression is performed on the $\ln(I_o/I)$ versus the path length data to determine the attenuation coefficient from the slope of the fitted line.

For the case of TCA the above method of calibration was not possible, since the TCA is a very strong plastisiser and the acrylic box would be destroyed had it been filled with TCA. For this reason a variation of this technique was performed using different diameter Pyrex glass beakers. The glass beakers were scanned along their diameter first empty and then full with TCA. Each measurement took 180s. The results are presented in Table 4 and the linear regression line is shown in Fig 8.

6 1st experiment

6.1 Experimental set-up

The experimental set-up for the first experiment is summarised in Table 4. It consisted of a saturated #30 sand matrix and an inclined layer of #16 sand with an angle of 7.5° to the horizontal. About 500ml of red TCA were injected with a constant head of 10cm.

Photographs of the spill are shown on Fig. 9 and the TCA saturation measurements with the γ-rays are plotted on Fig. 10 and 11. The saturation calculations using the γ-scan results are on Tables 5 and 6.

Notes:

1. For each measurement, the live time of the scan was 60s with 3 point repeats.
2. The points for the gamma scanning (Fig. 12) were selected to be as descriptive as possible. Directly under the injection point, measurements were made at one point in each sand type and one point in the lower sand interface. The same horizontal levels were scanned at 3 more columns, which were 6 inches apart. It would have been better to scan the whole tank in a fine grid before and after the DNAPL injection, but this is a very time consuming operation since it requires for the same γ-scanning set-up 180s=3 min per point.
3. An attempt was made to capture the dynamic phase of the experiment by scanning the column directly under the injection devise continuously overnight, starting at the time the injection began. The saturation measured by the γ-rays for this column is plotted in Fig. 13.

6.2 Observations

- Bubbles were observed in the water on top of the sand surface. These are attributed to the water in the tank not being properly de-aired and thus containing air. Once it sat for a while, bubbles started to form.
- The drainage taps at the two ends of the tank were initially closed at the beginning of the DNAPL injection. This resulted in pooling of the DNAPL on the soil surface. The head of the DNAPL was not sufficient to push it directly into the underlain sand and so it moved upwards. The problem was solved after the drainage taps were opened. More TCA was

added in the injection device in order to inject the predefined quantity of DNAPL (about 500ml), despite the pooling of the DNAPL on the sand surface. The added quantity was about 100ml. The pooled DNAPL is believed not to have had any influence on the experiment.

- Although both ends of the tank were kept at constant head at the same level, there was flow of water out of the tank only in the direction that the DNAPL was moving. The water was pushed in a piston-like manner by the TCA.
- No fingering was observed: the TCA moved as a continuous phase and no disappearances from the walls and re-appearances further down were noted.
- The DNAPL reached the fine sand lining of the walls of the tank (the downstream wall only) within only one hour after the beginning of the injection. This was a lot shorter than initially anticipated.
- The attempt to capture the dynamic phase of the experiment failed due to an electronics fault. γ-ray measurements taken during the injection and overnight, after the injection was stopped, may not be reliable. The electronics fault was discovered as the counts for the Cesium source were negative values. This does not necessarily mean that the Americium counts are also wrong, since the counts for the two sources are taken from different channels but the estimated saturation values should only be treated cautiously.

6.3 Discussion

- Various scales of heterogeneity affected the DNAPL flow greatly. In this specific experiment there were two different types of heterogeneity: (a) one was the coarse layer in the middle of the sand matrix, which was a fully defined heterogeneity and (b) the other was created during the "wet sand packing". The issue raised in this experiment refers to the unwanted heterogeneity, which was created during the sand compaction. These had random inclination to the horizontal and should not be in the matrix. Still, they affected the flow greatly, as it can clearly be seen from all the photographs (Fig. 9). Immediately below the injection point the DNAPL evolved and spread quite uniformly but the horizontal edges of the plume had the form of a spruce spreading at the interface of each compacted layer. The stratification observed within each compacted layer is due to the fine particles staying in suspension during the wet pouring and settling with slower rates than the rest of the heavier particles. These smaller particles created a very thin layer that had smaller porosity and was less permeable than the rest of the matrix. It is also

considered that the suspension of particles is accentuated by a tool used for compaction. It was a solid plastic plaque with no holes for drainage. Every time it was raised, suction was applied on the sand surface and even the bigger particles were lifted. This procedure increased the degree of stratification.

- The γ-system did not give a very good DNAPL saturation profile since only few points were scanned. Still, the saturation measured by the gamma rays is comparable to what was seen on the glass walls of the tank (Fig.9, 10 and 11). This means that TCA was not revealed by the γ-system at locations where it could not be seen on the glass walls.

Apart from all the above comments, the experiment was good, in the sense that it showed what was expected and also the packing proved to be good with no fingering observed.

7 2nd experiment

7.1 Experimental set-up

The set-up for the second experiment is summarised in Table 6. It consisted of a saturated #30 sand matrix with an inclined layer of #16 sand with an angle of 5° to the horizontal. About 500ml of red TCA were injected with a constant head of 10cm. Photographs from the spill are shown on Fig. 14 and the γ-scan results are plotted on Figs. 15 and 16. The calculations for these plots are listed on Table 7.

Notes:

1. The whole tank was scanned in a fine grid (about 100 points, shown in Fig. 17) once before and twice after the DNAPL injection.
2. The live time of the scans was 120s and each point was only scanned once (1 repeat). It is believed that by increasing the live time and decreasing the number of point repeats, the accuracy is improved and time is saved.
3. In this 2nd experiment it was decided to concentrate on acquiring one good set of data (either photographs or γ-scans). For this reason only photographs were taken during the dynamic phase of the experiment and the tank was scanned with the γ-rays only after the DNAPL had stopped moving fast.

7.2 Observations

- There was a leak in the injection system just after the injection started. The injection was immediately stopped and the system was fixed and set-up again. This resulted in pooling of TCA on the sand surface that was promptly removed. It is believed that no TCA migrated downwards before the injection restarted.
- The injection orifice was not placed exactly perpendicular.
- The shape of the plume on the front and the back wall were not the same. This can be attributed to the fact that the orifice of the injection devise was not precisely located along the longitudinal axis of the tank.
- Fingering was observed. The injected TCA initially moved within the sand in the centre of the tank and it did not appear on the walls of the tank. It then appeared on the tank walls at some downward locations. This is probably due to non-satisfactory packing of the sand, resulting in the sand not being uniform and homogenous.
- The tank was scanned on a very dense grid (see Fig. 17) so that better measurements than the ones from the 1st experiment would be taken. However, the time required to perform the whole scan was a problem with such a dense scanning pattern. The whole scan took approximately 6 to 7 hours.

7.3 Discussion

From the pictures and in general the observations it can be discussed that:

- The pattern of the TCA plume that appeared on the glass walls cannot lead to any conclusions on the fate and transport of the TCA in the sand due to fingering.
- No conclusion can be drawn from the gamma scans either.
- Only speculations can be made as to what caused such patterns of migration. The most probable reasons are:
  1. Inhomogeneous packing of sands (although the procedure followed was similar to the procedure in the 1st experiment)
  2. The non-centralised location of the injection point
  3. The start-stop-start form of the injection (in the very early stages) due to the initial malfunction of the injection device may have initiated preferential paths in the sand.

8 Discussion on issues raised

8.1 Safety issues

During the course of the experiments, several safety issues were raised in handling various materials. The materials of concern are:

1. Silicon glue: it was used extensively while the tanks were assembled to glue the gaskets to the tank frame and also to stop leaks after the tank was filled with water. The silicon glue has a very strong odour that causes nausea and dizziness. It is suggested that silicon glue be used in well-ventilated rooms.
2. Silica dust: while sand was transported, mixed with silt and then poured in the tanks, dust was produced and stayed in suspension for a while. Health and safety regulations require that dust masks are worn at all times when handling sand. The dust masks (paper masks) prevent the inhalation of the dust particles.
3. TCA: it has a very strong odour. It causes tiredness, nausea and it may also be carcinogenic. It should be handled with extreme care in a fume cupboard wearing protective gloves, glasses and clothing. Chemical masks (masks with special chemical filters) should be worn during handling. It is heavier than water so a thin layer of water can be poured over its top to prevent it from being in contact with the air.
4. Soltrol: it has low toxicity, but its vapours may cause tiredness. When in touch with the skin it causes hand burns. It is advised to use it in a well ventilated area wearing protective clothing (gloves etc).
5. Dyes: a commonly used dye for NAPLs is SUDAN, which is available in several different colours (red, black, and blue). This dye presents a serious health risk since it is a mutagen. The dye used in the laboratory at CU is the Automate Red dye that does not present such health risks. It should be noted that the Material and Safety Data Sheets in the UK did not stress the mutagenic effect of the Sudan dye.
6. Radioactive materials for the γ-rays attenuation system: the two sources used were Americium and Cesium. Badges measuring radioactivity should be worn at all times and checked regularly when working close to the sources and standing in front of the radioactive sources should be avoided.

8.2 Sand pouring techniques

The method of sand pouring used in the conducted experiments produced samples that were

not uniform. After the visit to the laboratory at CU, the literature was reviewed for various sand pouring techniques. The results of this review are summarised below:

- The literature on groundwater contamination, despite the fact that it involves filling tanks with sand, does not refer to the method of filling extensively.
- Literature on sand pouring techniques was found on the subjects of sand sample preparation for soil laboratory testing, calibration chambers for the testing and calibration of Cone Penetration Tests (CPT) and other in-situ testing methods and experimental set-ups looking into soil-structure interaction problems. The last two subjects are in particular the most related to the groundwater contamination tanks due to the large volume of soils involved.
- Most of the theories on sand pouring techniques are based on the early work by Kolbuszewski (1948).
- Tamping, compacting and vibrating techniques do not produce uniform samples (Cole 1967). Pouring (pluvial deposition) techniques produce more uniform samples. Two categories of pluviators have been found: the stationary one (Cole (1967), Fretti et al. (1995), Vaid et al. (1984), Magda (1993) and more) and the travelling pluviators (Cole (1967), Fretti et al. (1995) and more).
- According to Kolbuszewski (1948), the density of the sand packing is a function of the intensity of the deposition, the velocity of the deposition (flow rate), the acceleration on the deposition, the mean diameter of the sand particles and the mean density of the sand particles. Denser samples are obtained by increasing the height of fall, reducing the velocity of deposition (flow rate) and in the case of travelling pluviators, increasing the travelling velocity (Pallacqua, 1991)
- When sand is poured in water, its density is independent of the intensity of flow and the height of fall (Kolbuszewski, 1948). This means that no dense sample can be obtained when pouring through water.
- Following the findings of this literature search, other methods of filling the tank with sand should be used in future experiments in order to minimise unwanted heterogeneity.

8.3 Water used

The water used in both experiments was tap water, not de-aired. Air is dissolved in the tap water and it may affect the saturation measurements. A common de-airing procedure followed at CU was leaving the tap water in a bucket to stand for one or two days. When

bubbles form on the side walls, the water is considered de-aired. However, this method does not de-air the water completely. A strong vacuum pump along with continuous stirring of the water is needed, to remove all the air from the water.

Another point to be noted with the use of tap water is the high salt content. Although salts in the water should not affect the multiphase flow, it is recommended to use de-ionised (distilled) water for reproducible experiments.

8.4 Notes on the calculation of TCA saturation using the γ-rays measurements

For all the saturation calculations made during these experiments a path length value and a porosity value were required. The path length value was taken constant equal to 5.08cm. This value may be considered accurate because the tank is small and stiff and does not bulge.

The porosity value was assumed constant and equal to 0.5. This is only an assumption because it was not measured directly by taking samples or indirectly using the γ-system. Moreover, as discussed above, the sand was not homogeneous, so one porosity value characterising the whole of the tank is not satisfactory. For these reasons, the reported DNAPL saturation measurements should be looked qualitatively in comparison with the photographs taken.

9 Conclusions of the DNAPL experiments

The quality of these experiments was not satisfactory. They were conducted mainly for the educational purpose of performing DNAPL experiments. What was sought after was (a) training in the design of such experiments, (b) assembling such tanks, (c) pouring sand in the tank in different angles and most importantly (d) learning how to use the γ-rays attenuation system.

The following conclusions are drawn from the experiments:

- Even micro heterogeneities in the sand affect the flow of the DNAPL.
- Very carefull sand packing is needed to obtain good quality data in both pictures and γ-scans.
- It was not possible to take good digital photographs and at the same time scan the tank

using the γ-rays attenuation system.

- For reliable γ-scan results it is necessary to use de-aired water to minimise the gas content in the tank.
- The interface between the coarse sand layer and the undelying medium sand acted as a barrier to prevent further downward migration of the TCA. Once the TCA reaches the interface, it started migrating along the interface by gravity (the interface in both of these experiments was inclined).
- For more accurate calculation of the TCA saturation with the γ-rays attenuation system, it is necessary to take into account all the factors attenuating the γ-rays, namely the tank itself, the soil and the water. A precise knowledge of the porosity of the sand at each point is necessary.

10 References

Cole, ERL (1967), *Soils in the simple shear apparatus*, PhD Thesis at Cambridge University.

Compos, R (1997), *Multiphase experimental realizations of Dense Non Aqueous Phase Liquid spreading in saturated heterogeneous porous media*, MSc Thesis at the University of Colorado.

Fretti, C, DCF Lo Presti, and S Pedroni (1995), A pluvial deposition method to reconstitute well-graded sand specimens, *Geotechnical Testing Journal*, **18(2)**, pp. 292-298.

Illangasekare, TH, JL Ramsey, KH Jensen, and MB Butts (1995), Experimental study of movement and distribution of dense organic contaminants in heterogeneous aquifers, *Journal of Contaminant Hydrology*, **20**, pp. 1-25.

Kolbuszewski, JJ (1948), "An empirical study of maximum and minimum porosities of sands", In:*Proc. 2nd ICSMFE, Rotterdam 1948*, pp. 158-165.

Kueper, BH, and JI Gerhard (1995), Variablility of point source infiltration rates fro two-phase flow in heterogeneous porous media, *Water Resources Research*, **31(12)**, pp. 2971-2980.

Kueper, BH, and DB McWHorter (1992), The use of macroscopic percolation theory to construct large scale capillary pressure curves, *Water Resources Research*, **28(9)**, pp. 2425-2436.

Magda, W (1993), "Control of sand specimen density by sand pouring technique", In:*Eleventh Southeast Asian Geotechnical Conference, Singapore 1993*, pp. 159-164.

Passalacqua, R (1991), A sand spreader used for the reconstitution of granular soil models, *Soils and Foundations*, **31(2)**, pp. 175-180.

Poulsen, MM, and BH Kueper (1992), A field experiment to study the behaviour of Tetrachloroethylene in unsaturated porous media, *Environmental Science and Technology*, **26(5)**, pp. 889-895.

Vaid, YP, and D Negussey (1984), Relative density of pluviated sand samples, *Soils and Foundations*, **24(2)**, pp. 101-105.

TABLES

Table 1: Measurements and calculations for the attenuation of the americium source by the Trichloroethane (TCA).

Size of Pyrex Beaker	ml	250	400	600	800
Beaker diameter = path length	**mm**	**68**	**77**	**90**	**100**
Empty beaker	I_o	3305277	3109561	3012037	3409626
TCA-full beaker	I	162138	114856	70115	47890
ln (I_o / I)		3.014828	3.298558	3.760235	4.265451

Table 2: Properties of the sands used in the experiments. (Table from Compos (1997), where the Brooks-Corey data are from air-water capillary pressure-saturation curves).

Sand type	#16	#30	#70
K (m/day)	694.1	171.4	21
Intrinsic permeability k_w (m^2)	9.17 E-10	2.26 E-10	2.77 E-11
Mean grain size (mm)	1.08	0.51	0.20
Brooks-Corey λ	3.5	2.1	1.9
Residual water saturation S_r	0.07	0.26	0.30

Table 3: Physical and chemical properties of Trichloroethane (TCA).

Density	1.32 g/cm^3
Viscosity	1.20 cP
Solubility	0.07 g/100gH_2O
Vapour pressure	124.6 torr

Table 4: Experimental set-up for the 1st experiment.

Sand used in the matrix	#30
Sand used in the layer	#16
Inclination of the sand layer	~7.5° to the horizontal
Filling of the tank	Wet: sand poured over a water height of approximately 10cm and tamped for compaction.
Quantity of TCA used	500ml
Duration of spill	~1 hour
Water used	Not deaired
Locations of γ-ray scanning	3 columns x 3 rows = 9 points only points shown on Fig 12
Definition of scanning points	each point=middle of cell 1 cell=(2x1)inch=(5.08x2.54)cm
γ-ray scanning configuration	60s scan x 3 repeats for each point

Table 5: **Calculations for the γ-scan results of the 1st experiment.**

EXPERIMENT 1

Live Time= 60s

Spill: December 4, 1997

Calibration scan: December 3, 1997
Measurment #1 : December 5, 1997

Una	Unc
0.0387	0.056

Path Length, x	
5.08	5.77

Porosity, n
0.43

Calibration Scans

Water saturated packed tank

	Column 4	7	10	13	
Row	Am	Am	Am	Am	
4	28031	28096.7	27299.7	27548	4
8	25859	25992.7	25806	26487	8
12	24554	24537.7	24452	25330.3	12
16	26465	25320.3	24849.3	26375.3	16

Equation used for the sa

1st set Measurement Scans

	4	7	10	13	
Row	Am	Am	Am	Am	
4	25178.3	28268.7	27272	27741.7	4
8	24633.7	25993	25836.3	26217.3	8
12	24031.7	23351.7	24493.7	25177.3	12
16	26473.3	25063.7	24716.7	26248.3	16

Saturations

	4	7	10	13	
Row	Am	Am	Am	Am	
4	127.0	-7.2	1.2	-8.3	4
8	57.4	0.0	-1.4	12.1	8
12	25.4	58.6	-2.0	7.2	12
16	-0.4	12.1	6.3	5.7	16

Table 6: **Calculations for the γ-scan results of the 1st experiment.**

EXPERIMENT 1

Live Time= 60s

Spill: December 4, 1997

Calibration scan: December 3, 1997
Measurment #2: December 8, 1997

Una	Unc	Path Length, x		Porosity, n
0.0387	0.056	5.08	5.77	0.43

Calibration Scans

Water saturated packed tank

	Column 4	7	10		13	
Row	Am	Am	Am	Cs	Am	
4	28031	28096.7	27299.7		27548	4
8	25859	25992.7	25806		26487	8
12	24554	24537.7	24452		25330.3	12
16	26465	25320.3	24849.3		26375.3	16

2nd set Measurement Scans

	4	7	10	13	
Row	Am	Am	Am	Am	
4	25415	28437	27192.7	27548.7	4
8	24633	25665.7	25814.3	26076	8
12	24358	23583.7	24559.7	24810	12
16	26156	24721.7	24764.7	26281	16

Saturations

	4	7	10	13	
Row	Am	Am	Am	Am	
4	115.9	-14.2	4.6	0.0	4
8	57.5	15.0	-0.4	18.5	8
12	9.5	46.9	-5.2	24.6	12
16	13.9	28.3	4.0	4.2	16

Table 7: Experimental set-up for the 2nd experiment.

Sand used in the matrix	#30
Sand used in the layer	#16
Inclination of the sand layer	~5° to the horizontal
Filling of the tank	Wet: sand poured over a water height of approximately 10cm and tamped for compaction.
Quantity of TCA used	500ml
Duration of spill	~1 hour
Water used	Not deaired
Locations of γ-ray scanning	Most of the tank on a grid of 5.08x2.54cm points shown on Fig 17.
Definition of scanning points	each point=middle of cell 1 cell=(2x1)inch=(5.08x2.54)cm
γ-ray scanning configuration	120sec scan x 1 repeat for each point

EXPERIMENT 2

Live Time= 120s

Spill: December 12, 1997

Calibration: December 11, 1997
Measurment #1: December 12, 1997
Measurment #2: December 14, 1997

Una	Unc	Path Length, x		Porosity, n
0.387	0.056	5.08	6.77	0.5

Calibration Scans

Water saturated packed tank

Row	1 Am	1 Ca	2 Am	2 Ca	3 Am	3 Ca	4 Am	4 Ca	5 Am	5 Ca	6 Am	6 Ca	7 Am	7 Ca
1					55220		55142		57204		54480		55148	
2					55592		54631		54758		54290		53695	
3					56806		54860		55102		53806		53777	
4					55949		54700		53720		53988		53212	
5					53314		52838		52869		51822		51784	
6					51428		50112		50233		50294		49394	
7					52936		52820		51468		51396		51309	
8					51460		50848		48884		48070		46989	
9					53431		52617		51533		51347		50340	
10					52576		50798		50330		48906		48917	
11					52613		50745		52012		47587		48513	
12					50696		50006		50743		49651		48507	
13					51372		51607		51966		48095		50084	
14					52835		51334		50727		49022		48052	
15					53409		52449		51841		51181		50299	
16									52914		53602		51676	
17														
18														

Column

Row	8 Am	8 Ca	9 Am	9 Ca	10 Am	10 Ca	11 Am	11 Ca	12 Am	12 Ca	13 Am	13 Ca	14 Am	14 Ca	15 Am	15 Ca	16 Am	16 Ca		
1																			1	
2																			2	
3																			3	57.54
4																			4	55
5																			5	52.46
6	50581		50214		50796														6	49.92
7	51316		51195		50966		51315		51167		52639								7	47.38
8	47897		47554		49692		49441		50026		53151								8	44.84
9	50821		50227		50632		49414		49886		50172		52195						9	42.3
10	48064		48484		51486		49763		50646		53758		54655		57539				10	39.76
11	49519		49420		49496		49548		50141		51161		54345		58663		56758		11	37.22
12	48425		48740		49228		49621		49878		49611		52302		58700		54949		12	34.68
13	48815		48200		48214		48462		50255		49867		53027		58068		57767		13	32.14
14	49634																		14	29.6
15	51502																		15	27.06
16																			16	24.52
17																			17	21.98
18																			18	19.44
																				16.9

1st set Measurement Scans

Row	1 Am	1 Ca	2 Am	2 Ca	3 Am	3 Ca	4 Am	4 Ca	5 Am	5 Ca	6 Am	6 Ca	7 Am	7 Ca
1														
2														
3														
4			56794		53738		50414		53617					
5			54223		50750		49729		51275					
6			53968		49861		48347		49272		50222		50023	
7			54908		48589		51268		51058		51428		51572	
8			53366		48826		49596		47854		48446		47523	
9			55961		51371		50462		50435		51055		50759	
10			52599		49942		47627		47602		48263		48945	
11			53197		50712		49267		46077		46667		45904	
12			52807		50874		51620		48439		44976		47215	
13			54732		51450		53489		49418		48847		49921	
14			55529		52196		53340		50428		50009		49047	
15			56635		51597		52790		51466		50823		50761	
16			53706		50432		52823		53082		51072		51661	
17			52619		50185		51156		51763					
18			53329		52412		51548		53002					
19			53067		50474		52786		52574					

Row	8 Am	8 Ca	9 Am	9 Ca	10 Am	10 Ca	11 Am	11 Ca	12 Am	12 Ca	13 Am	13 Ca	14 Am	14 Ca	15 Am	15 Ca	16 Am	16 Ca		
1																			1	
2																			2	
3																			3	
4																			4	55
5																			5	52.46
6																			6	49.92
7																			7	47.38
8																			8	44.84
9																			9	42.3
10					51453										57190				10	39.76
11					45671										57488				11	37.22
12															51797				12	34.68
13																			13	32.14
14																			14	29.6
15																			15	27.06
16																			16	24.52
17																			17	21.98
18																			18	19.44
19																			19	16.9

Saturations

Row	1 Am	1 Ca	2 Am	2 Ca	3 Am	3 Ca	4 Am	4 Ca	5 Am	5 Ca	6 Am	6 Ca	7 Am	7 Ca
1														
2														
3														
4					4.1		8.3		0.4					
5					6.0		6.2		3.1					
6					5.0		3.6		2.0		0.1		-1.3	
7					5.8		3.0		0.8		-0.1		-0.5	
8					5.2		2.5		2.2		-0.8		-1.1	
9					4.0		4.3		2.2		0.8		-0.8	
10					5.2		6.8		5.7		1.4		-0.1	
11					3.7		3.0		12.3		2.0		5.8	
12					-0.4		-3.2		4.7		10.5		2.7	
13					-0.2		-3.6		5.1		-1.8		0.3	
14					0.9		-3.9		0.8		-2.0		0.0	
15					3.5		-0.7		0.7		0.7		-0.8	
16									-0.3		4.8		0.0	
17														
18														
19														

Row	8 Am	8 Ca	9 Am	9 Ca	10 Am	10 Ca	11 Am	11 Ca	12 Am	12 Ca	13 Am	13 Ca	14 Am	14 Ca	15 Am	15 Ca	16 Am	16 Ca		
1																			1	
2																			2	
3																			3	
4																			4	
5																			5	
6																			6	
7																			7	
8																			8	
9																			9	
10															8.8				10	
11					8.2										2.1				11	
12															12.7				12	
13																			13	
14																			14	
15																			15	
16																			16	
17																			17	
18																			18	
19																			19	

Table 8: calculations for the TCA saturation using the gamma scan results for the 2nd experiment

2nd Measurement Scans

Row	1 Am	1 Cs	2 Am	2 Cs	3 Am	3 Cs	4 Am	4 Cs	5 Am	5 Cs	6 Am	6 Cs	7 Am	7 Cs	8 Am	8 Cs	9 Am	9 Cs	10 Am	10 Cs	11 Am	11 Cs	12 Am	12 Cs	13 Am	13 Cs	14 Am	14 Cs	15 Am	15 Cs	16 Am	16 Cs		
1																																	1	
2																																	2	
3			55779		55291		55527		54046																								3	57.64
4			55236		55127		49964		53872		53884		53847		53268		53869		52894														4	55
5			53829		49652		49685		49891		52008		51918		51289		51763		50703														5	52.46
6			52088		48507		48453		48281		50114		49448		50476		50620		50953		51627												6	49.92
7			53518		49134		51164		50175		51268		51520		51188		50827		50868		51891								54947				7	47.38
8			52110		48904		49061		47982		47482		47190		47766		47790		48922		49793		51127						53418				8	44.84
9			54999		50470		50422		50469		51347		50414		50043		50253		50258		50027		50291		50345		52341						9	42.3
10			52081		49014		47188		48591		47903		48095		47999		48582		50854		50743		50567		53415		54047						10	39.76
11			52993		50815		48930		47826		45702		45844		47290		48066		47395		48099		48934		50951								11	37.22
12			52776		50504		51014		47399		41481		46824		42737		43714		45164		42999		43044										12	34.66
13			54399		51139		52706		46635		48218		50364		47824		48265		48219		49335		50195										13	32.14
14			53267		52187		52501		50099		49997		49242		49297		49178		50394														14	29.6
15			53756		51745		52444		52078		51983		50635		50123		49567		50099														15	27.06
16			53081		49419		53032		51941		52745		51266		49864		49980		50318														16	24.52
17			52025		50557		50634		50717																								17	21.98
18			52840		51998		50953		51492																								18	19.44
19																																	19	16.9

Saturations

Row	1 Am	1 Cs	2 Am	2 Cs	3 Am	3 Cs	4 Am	4 Cs	5 Am	5 Cs	6 Am	6 Cs	7 Am	7 Cs	8 Am	8 Cs	9 Am	9 Cs	10 Am	10 Cs	11 Am	11 Cs	12 Am	12 Cs	13 Am	13 Cs	14 Am	14 Cs	15 Am	15 Cs	16 Am	16 Cs		
1																																	1	
2																																	2	
3					2.9		-1.2		2.0																								3	
4					1.5		0.2		-0.3		0.2		-1.2																				4	55
5					7.2		8.9		8.9		-0.4		-0.8																				5	52.46
6					5.9		3.4		4.0		0.4		-0.1		0.2		-0.8		-0.3														6	49.92
7					7.6		3.2		2.8		0.3		-0.4		0.3		0.7		0.3		-1.1												7	47.38
8					5.2		3.6		1.9		1.3		-0.4		0.3		-0.5		1.6		-0.7		-0.2										8	44.84
9					5.8		4.3		2.1		0.0		-0.1		1.2		-0.1		0.8		-1.3		-0.8		-0.4		-0.3						9	42.3
10					7.1		7.5		3.6		2.1		1.7		0.1		-0.2		1.7		-2.0		0.2		0.7		1.1						10	39.76
11					3.5		3.7		0.0		4.1		5.8		4.7		5.4		4.4		3.0		2.6		0.6								11	37.22
12					0.4		-2.0		0.9		18.7		4.0		12.7		11.1		5.8		13.0		13.1										12	34.66
13					0.6		-2.1		11.0		-0.9		-0.6		2.1		-2.2		0.0		-1.8		6.1										13	32.14
14					0.9		-2.2		1.3		-1.4		-0.4		1.1																		14	29.6
15					3.2		0.0		-0.5		-1.0		-0.7		2.9																		15	27.06
16									1.0		1.6		0.9																				16	24.52
17																																	17	21.98
18																																	18	19.44
19																																	19	16.9

Table 8: calculations for the TCA saturation using the gamma scan results for the 2nd experiment

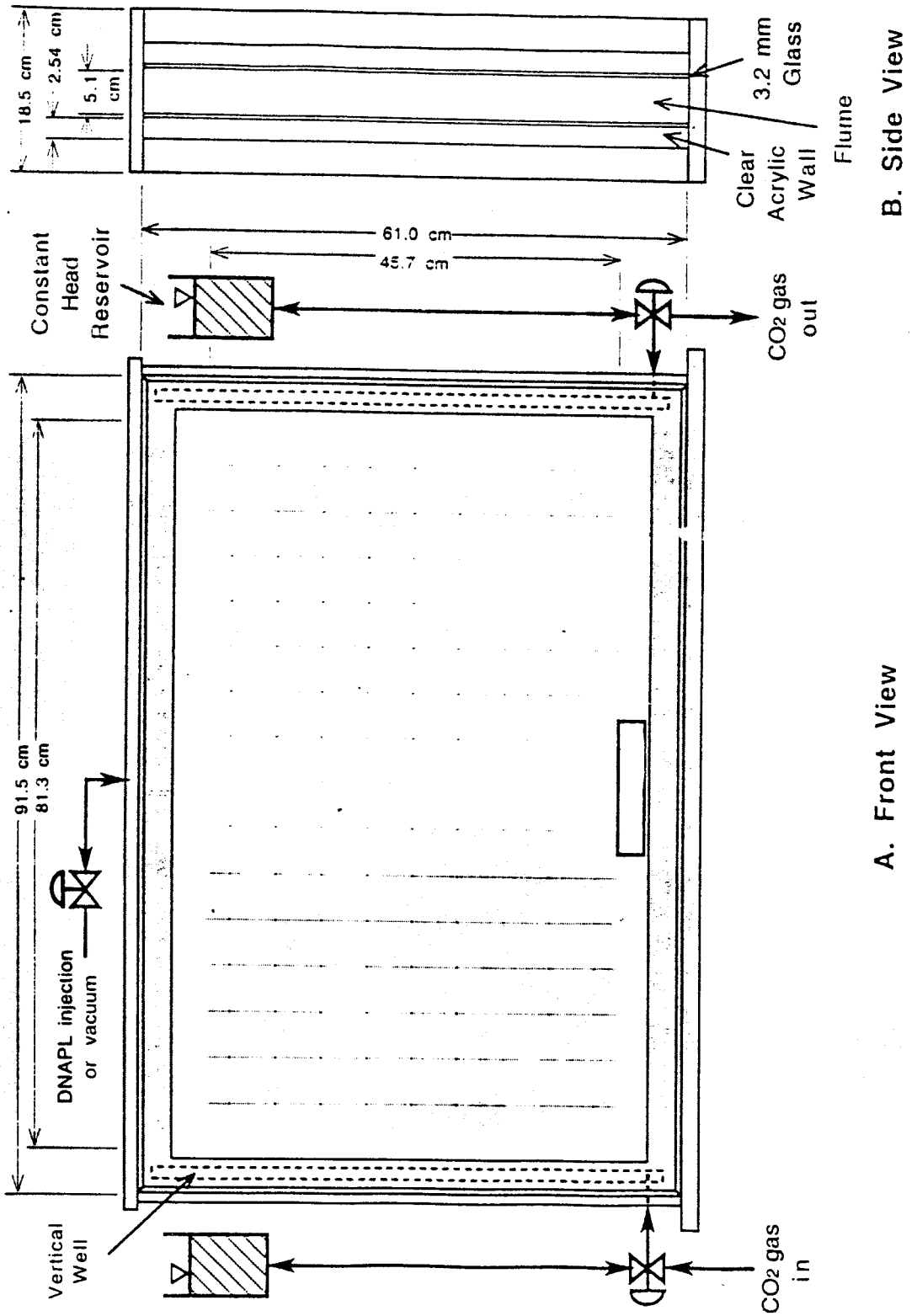

Figure 1: A schematic of the tank used (from Compos, 1997).

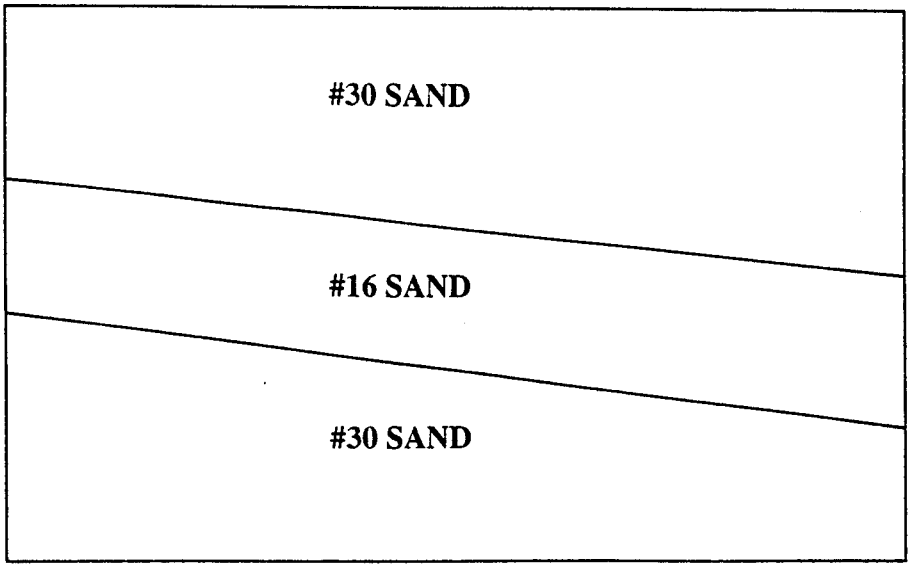

Figure 2: The sand configuration used.

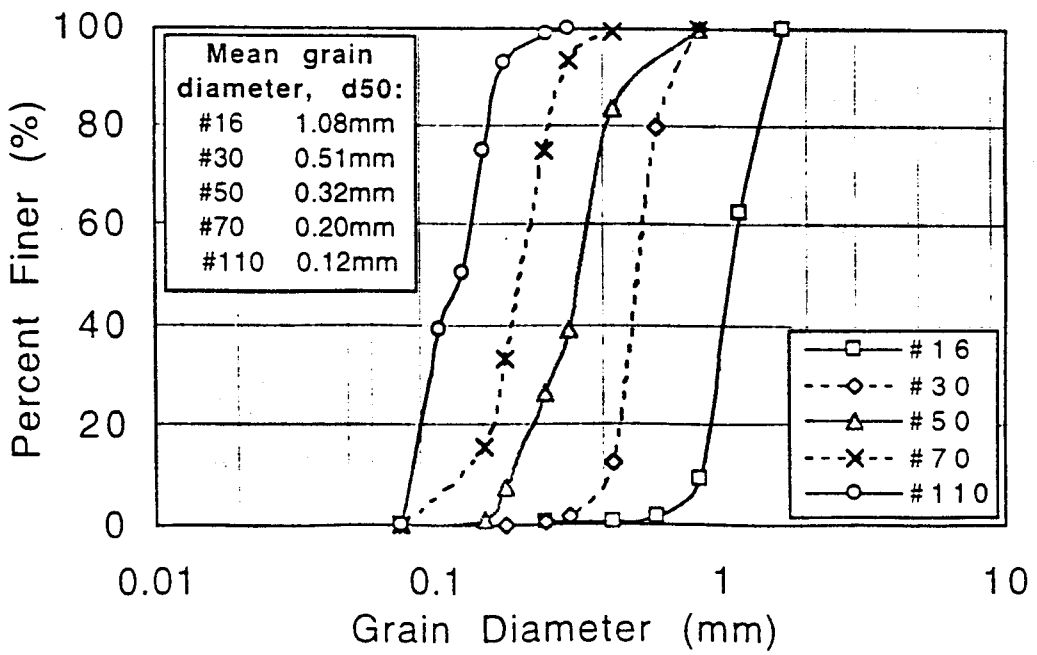

Figure 3: Grain Size distributions for the sands used (#16 and #30), from Compos (1997).

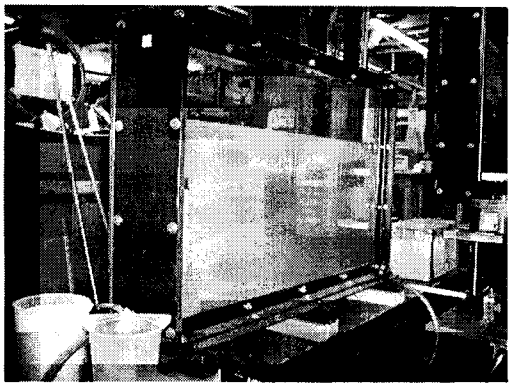

(a) Filling of the tank after the inclined coarse layer has been poured. The top fuzzy layer is coloured water.

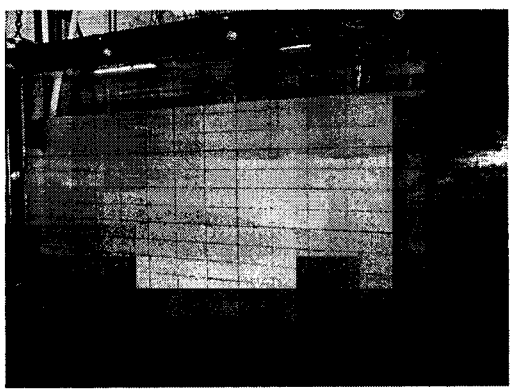

(b) Filling of the tank, towards the end of the procedure.

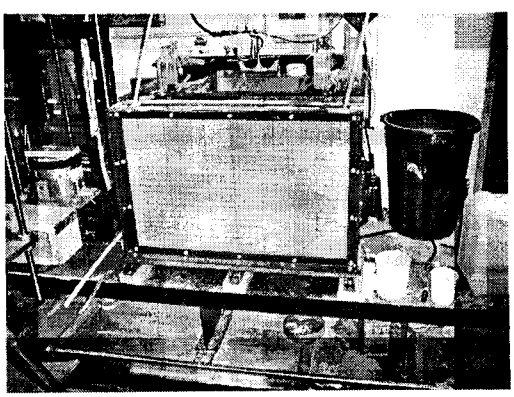

(c) The full tank: the inclined coarse layer can be seen as well as the lining of the walls with the fine sand.

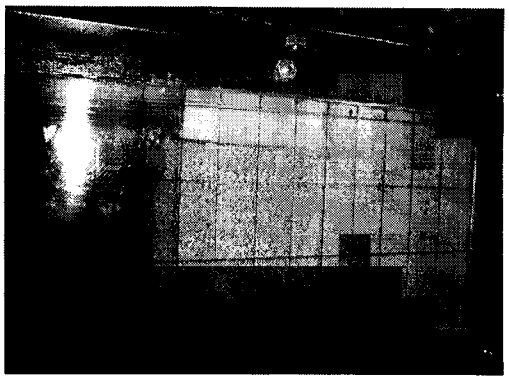

(d) Detail of the procedure for the lining of the side walls of the tank with fine sand. The plastic partition used can also be seen. Care must be taken for the level of the sand behind the partition (fine sand) to be at approximately the same level as the sand level in the main area in the tank. Otherwise, flow of sand occurs, which results in lenses of either fine sand in the medium or of medium sand in the fine. Such lenses can also be seen in this picture.

Figure 4: Filling of the tank with sand

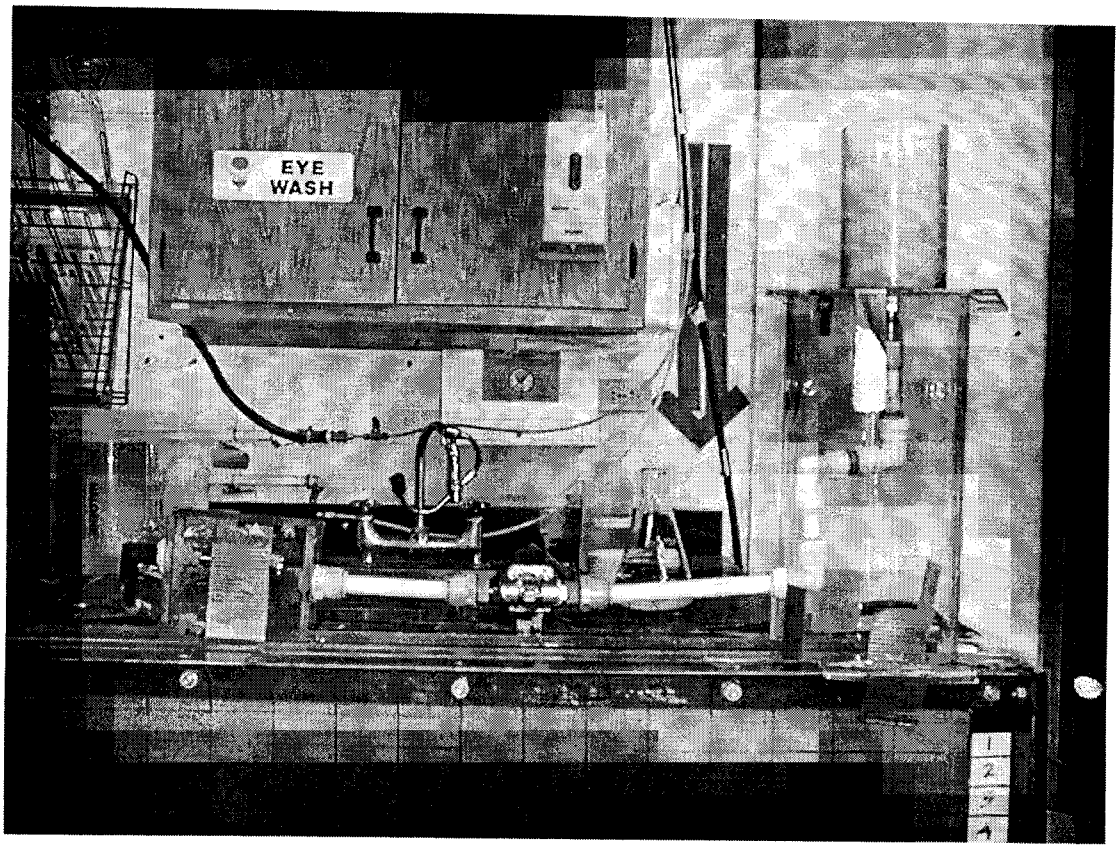

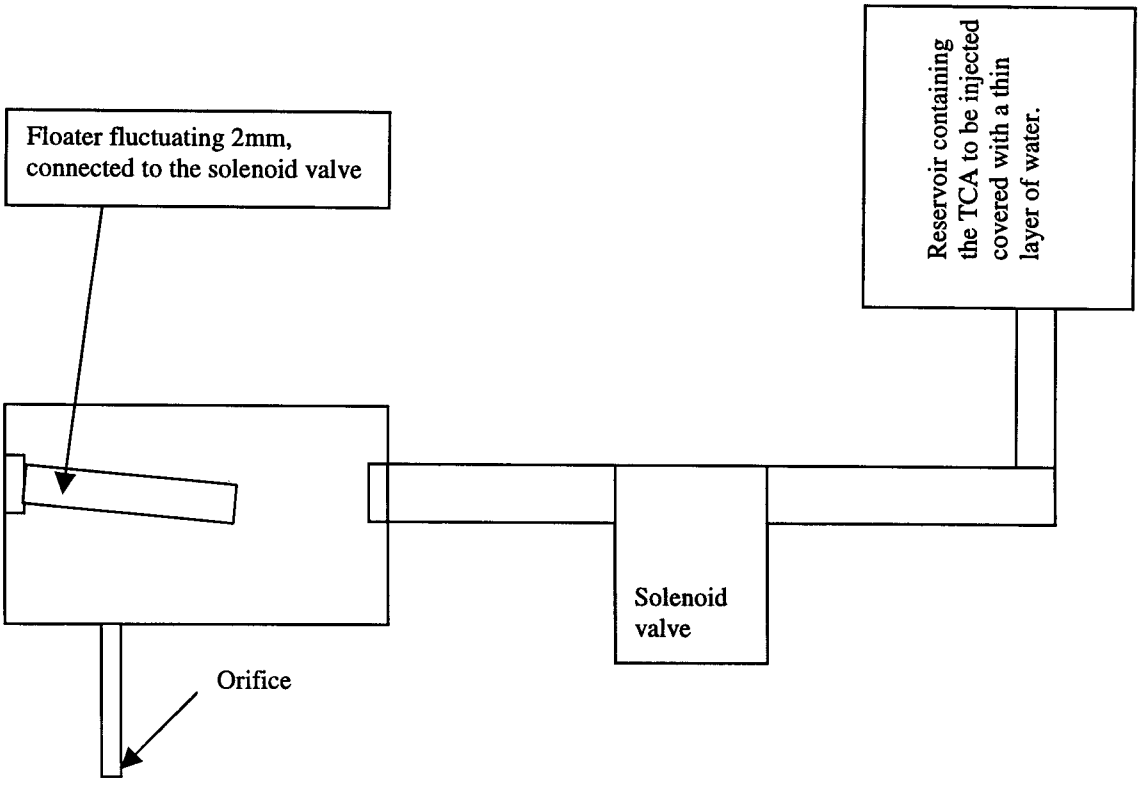

Figure 5: The injection device.

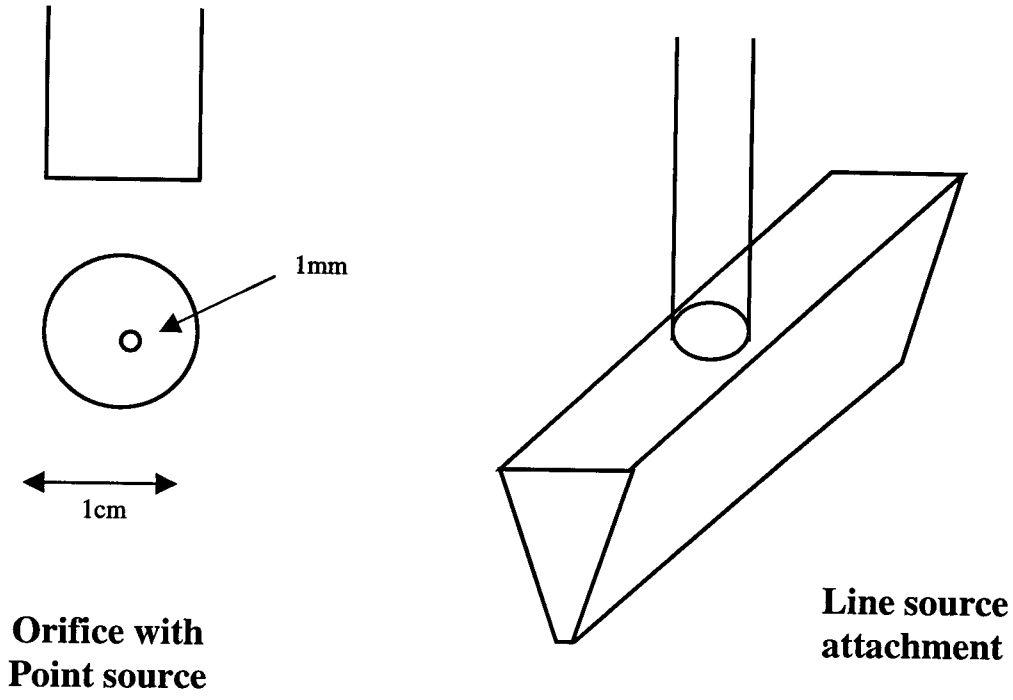

Figure 6: Orifice for the point source and attachment for the line source.

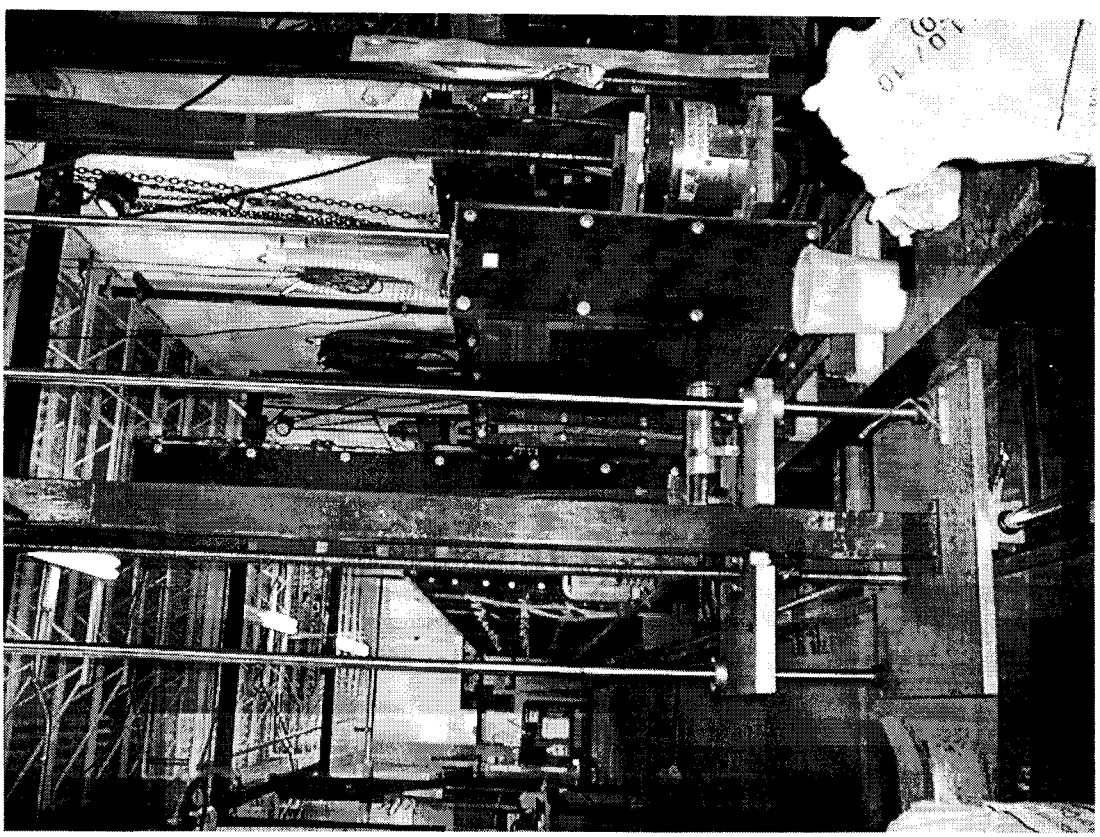

Figure 7: The tank with the gamma rays attenuation system.

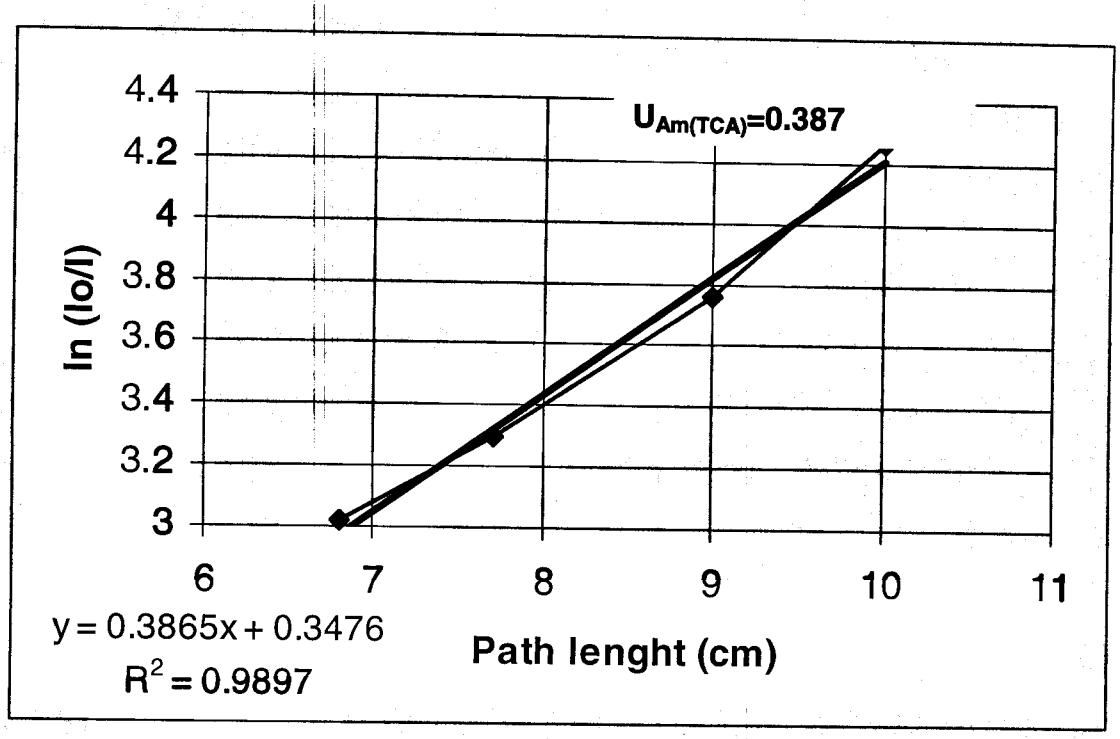

Figure 8: Linear regression for the calibration of the TCA. The lumped attenuation coefficient of the TCA is 0.387.

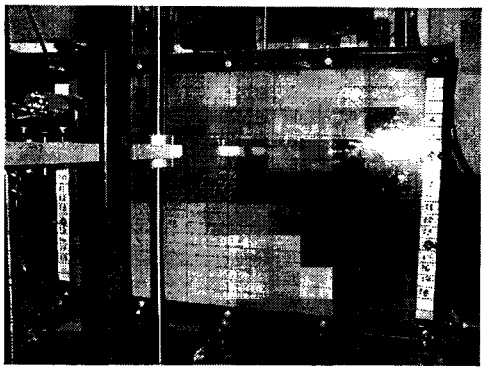

9mins and 56 sec

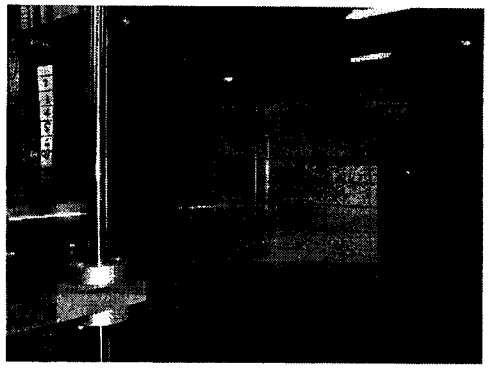

16mins and 41sec

13mins and 09sec

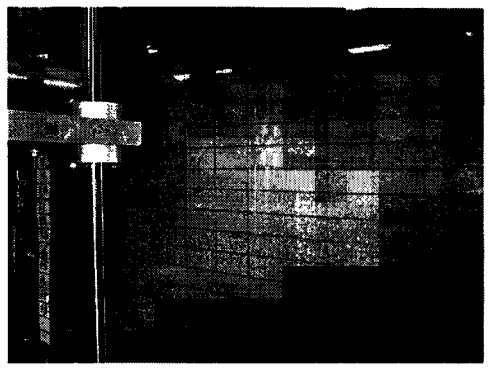

18mins and 09sec

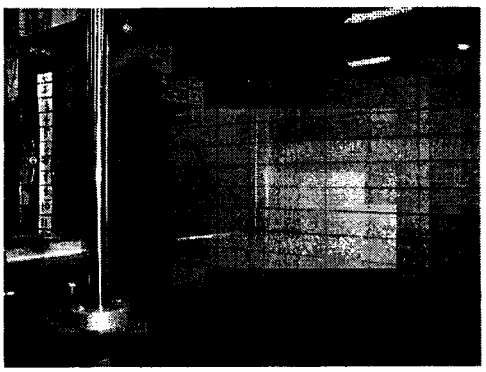

13mins and 42sec

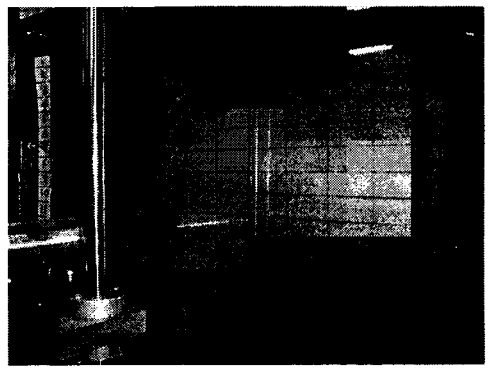

20mins and 25sec

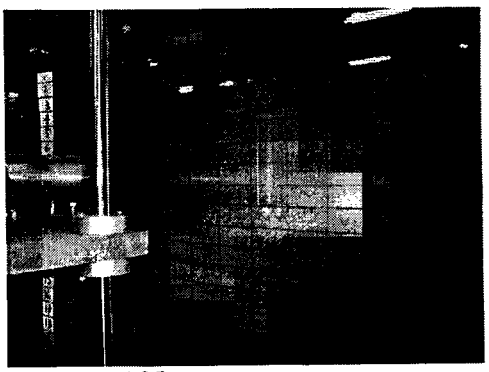

14mins and 35sec

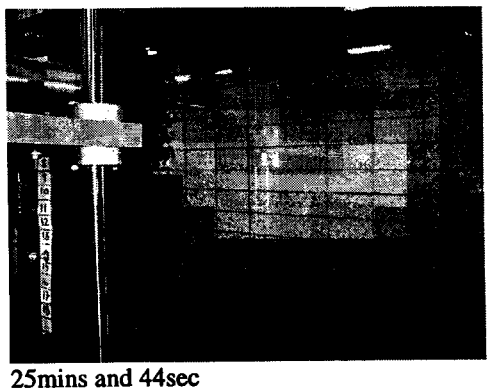

25mins and 44sec

Figure 9: The spill of the 1st experiment.

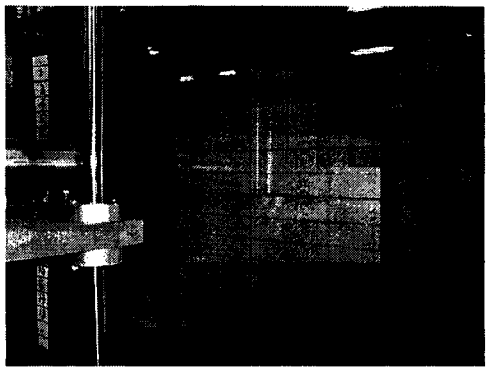

26 min and 19 sec

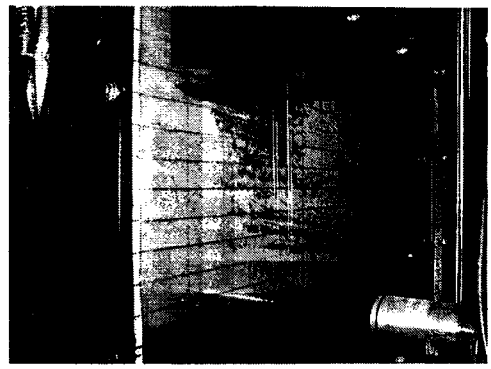

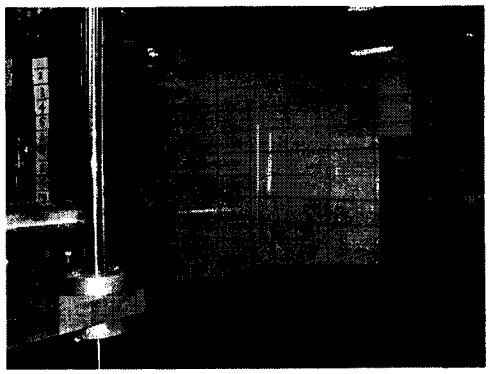

27 min and 47 sec

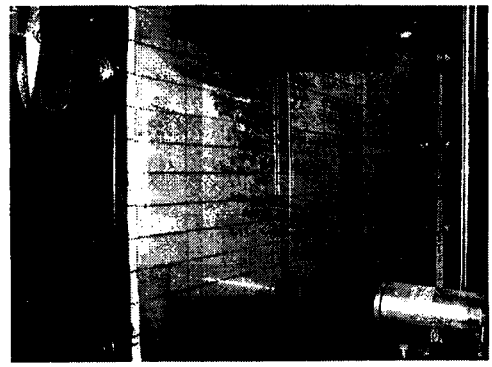

49 min and 30 sec

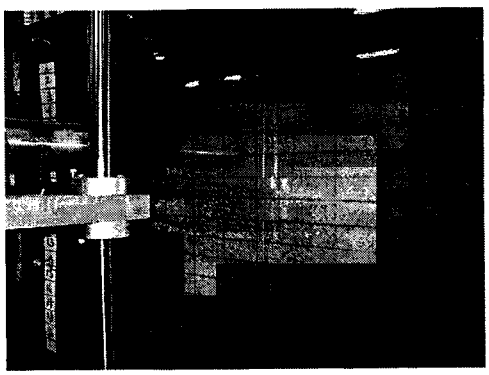

31 min

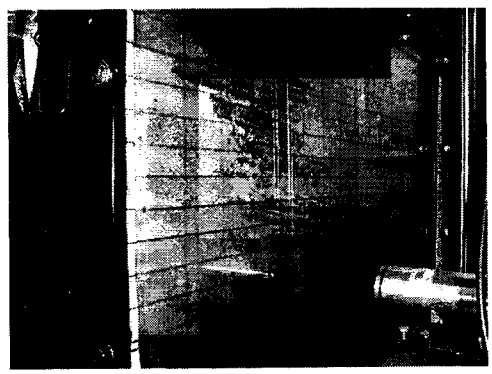

56 min

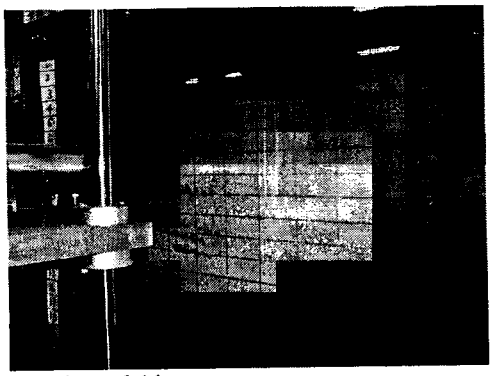

42 min and 11 sec

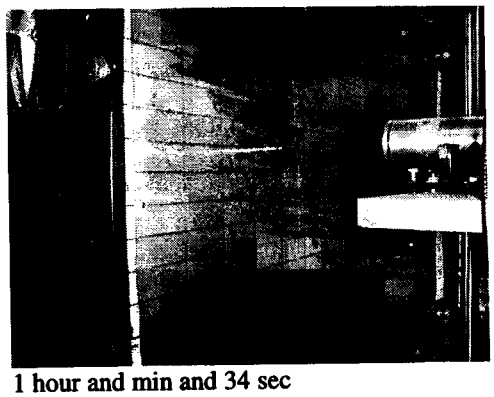

1 hour and min and 34 sec

Figure 9: The spill of the 1st experiment.

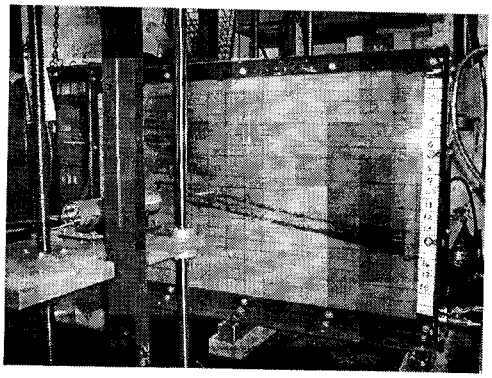

1 hour and 22 min and 30 sec

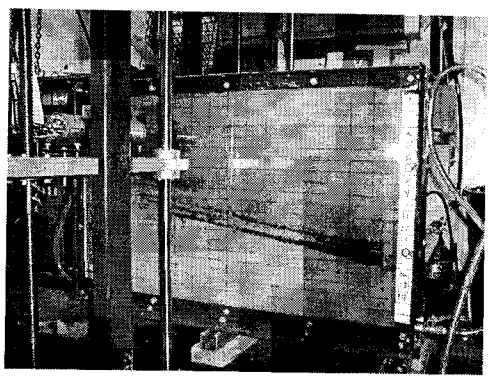

1 hour and 40 min

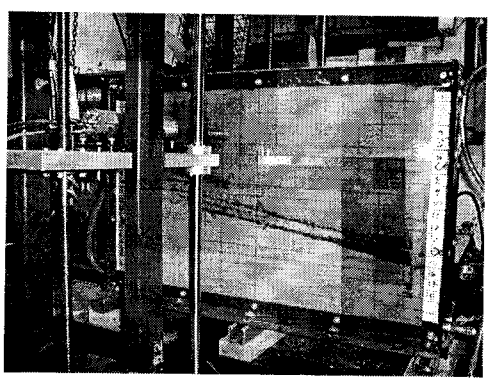

1 hour and 52 min and 27 sec

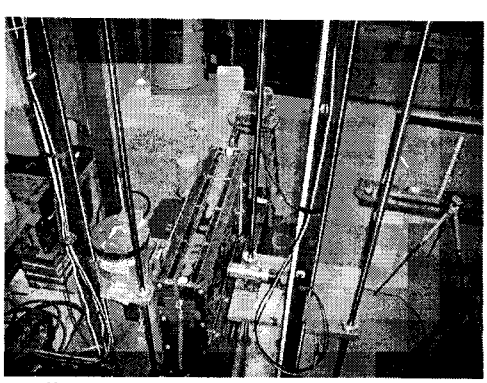

pooling on the top of the tank

Figure 9: The spill of the 1st experiment.

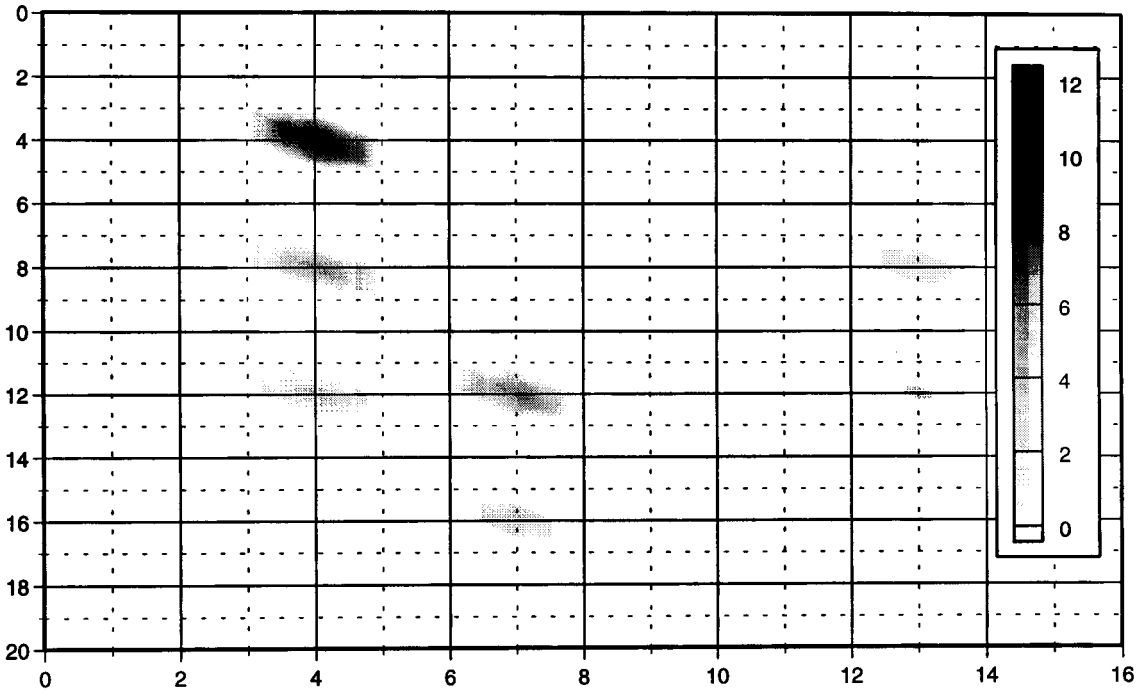

Figure 10: DNAPL saturations one day after the end of the injection of the 1st experiment.

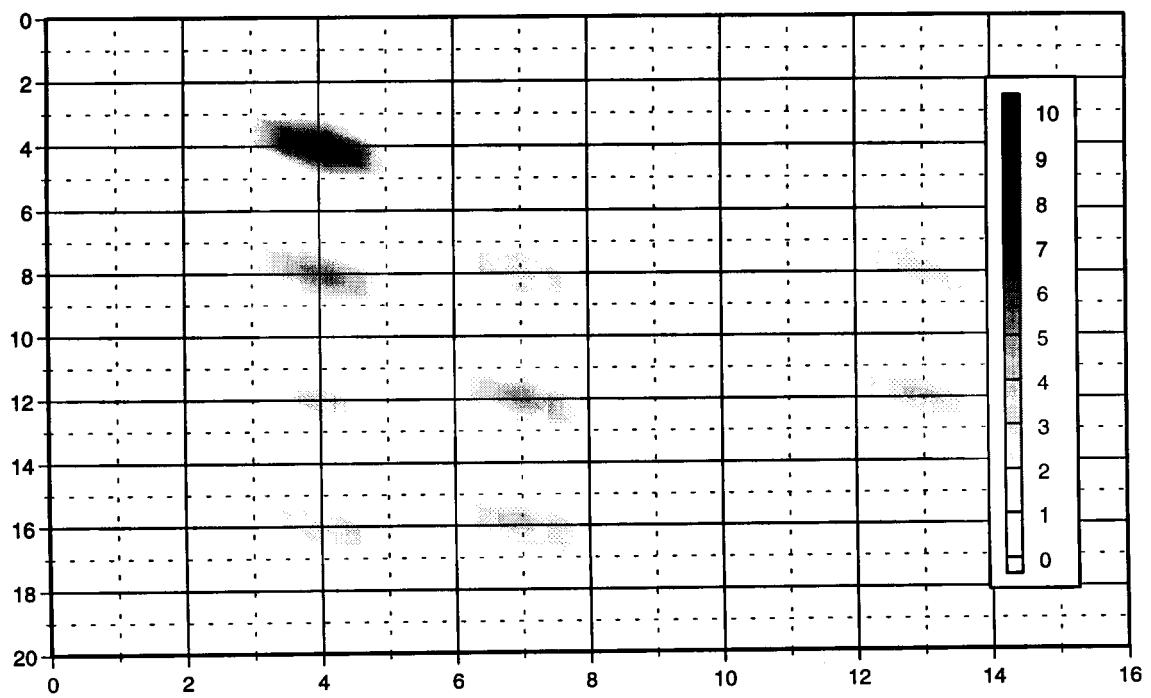

Figure 11: DNAPL saturations four days after the end of the injection of the 1st experiment.

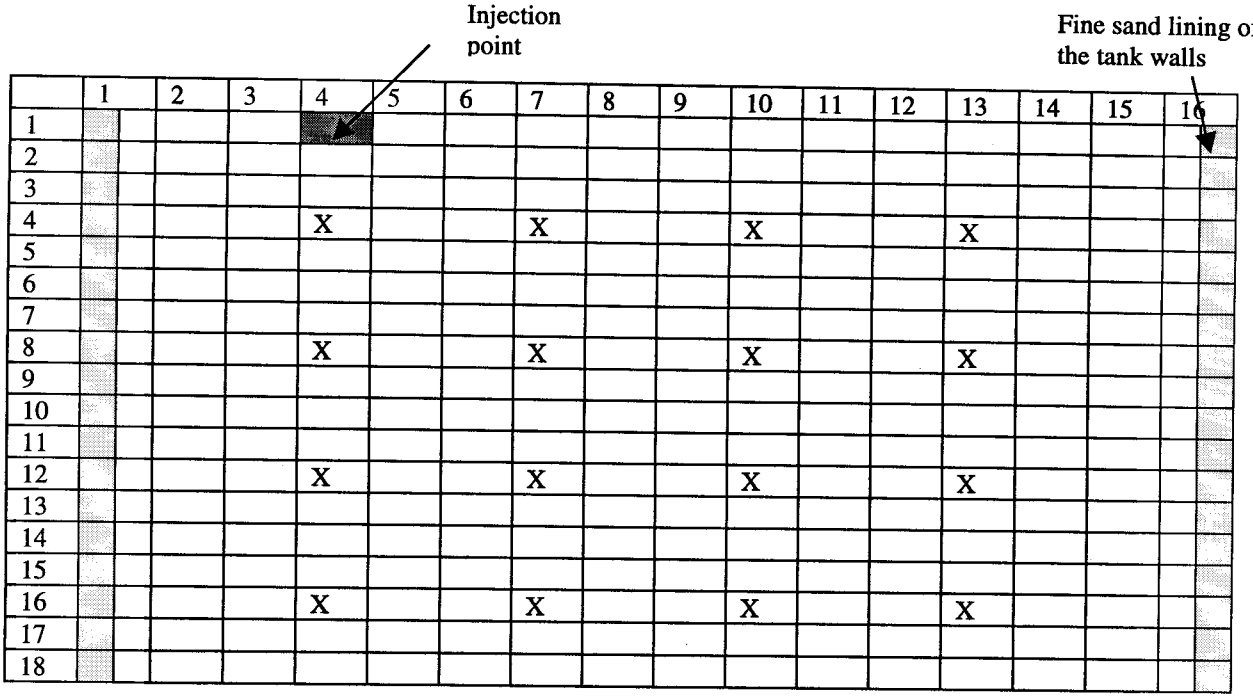

	1	2	3	4	5	6	7	8	9	10	11	12	13	14	15	16
1																
2																
3																
4				X			X			X			X			
5																
6																
7																
8				X			X			X			X			
9																
10																
11																
12				X			X			X			X			
13																
14																
15																
16				X			X			X			X			
17																
18																

Figure 12: With X are marked the locations in the tank, where γ-rays scans were performed during the 1st experiment.

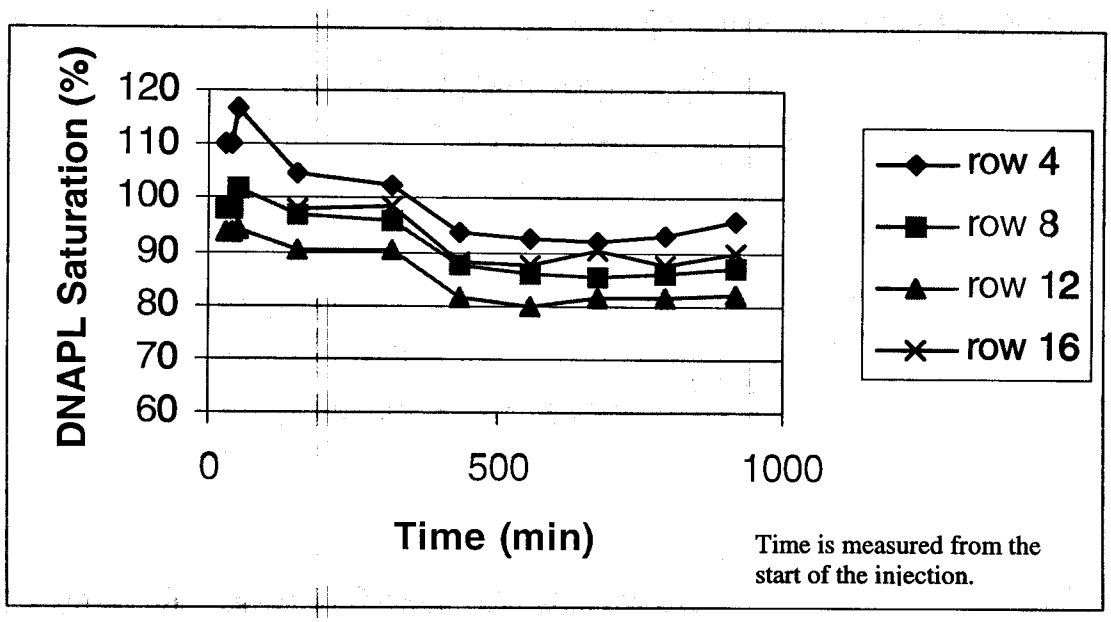

Figure 13: DNAPL saturations in column 4 (directly under the injection devise) measured with the γ-rays attenuation system during the dynamic phase of the 1st experiment (points with saturation values over 100% should not be considered, and are attributed to measurement errors).

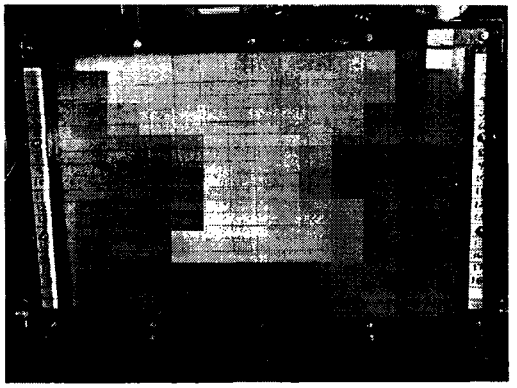

6 min 16 sec

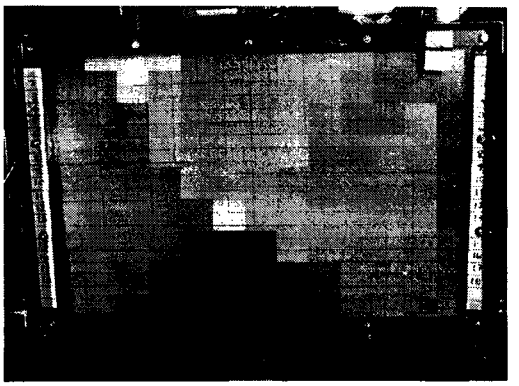

18 min 45 sec

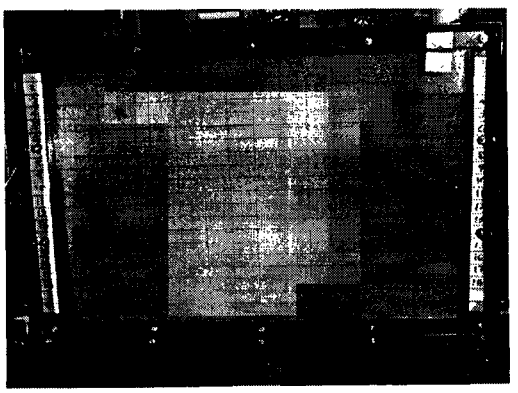

9 min 30 sec

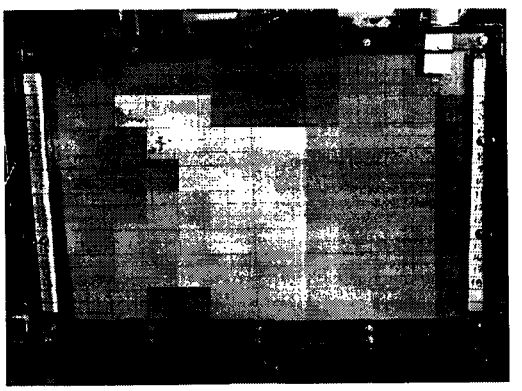

29 min 30 sec

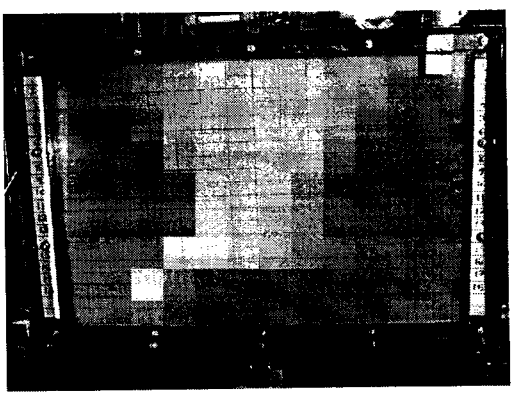

16 min 32 sec

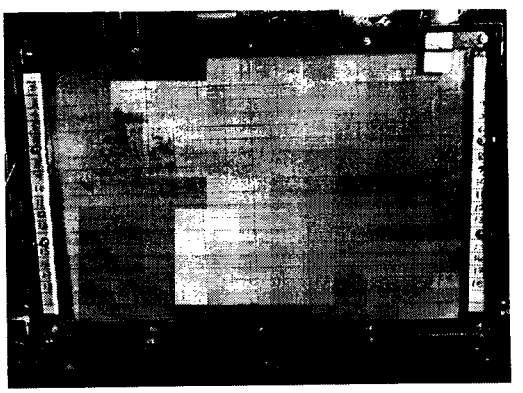

37 min 42 sec

Figure 14: The spill of the TCA in the 2nd experiment

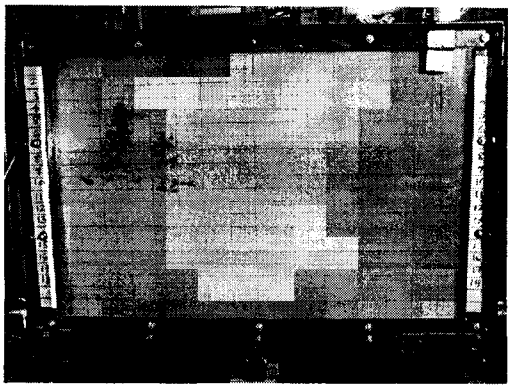

41 min 30 sec

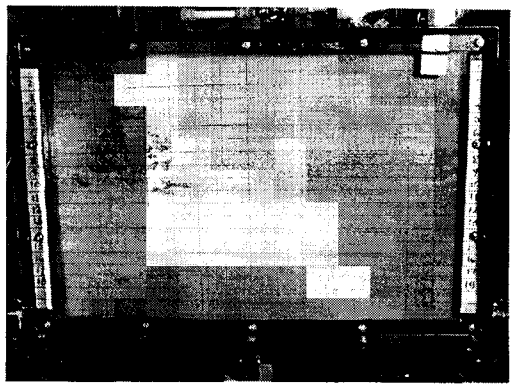

1 hour

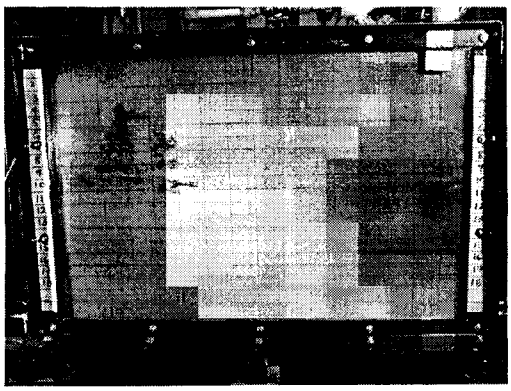

49 min 45 sec

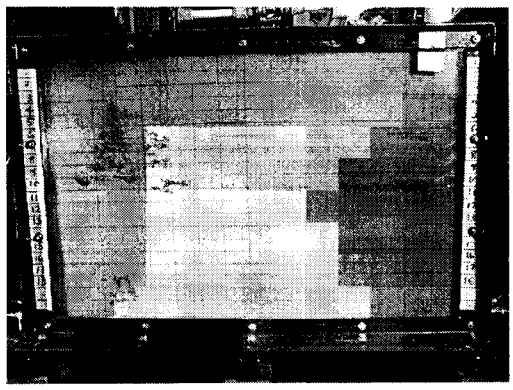

1 hour 8 min

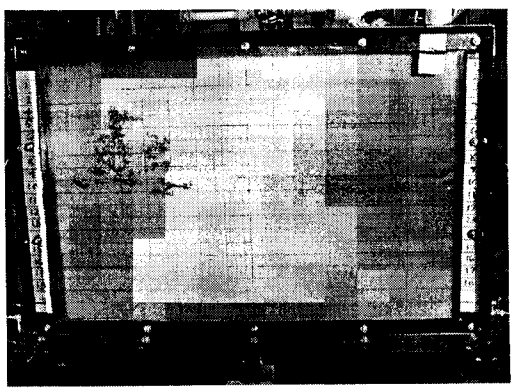

57min 15 sec

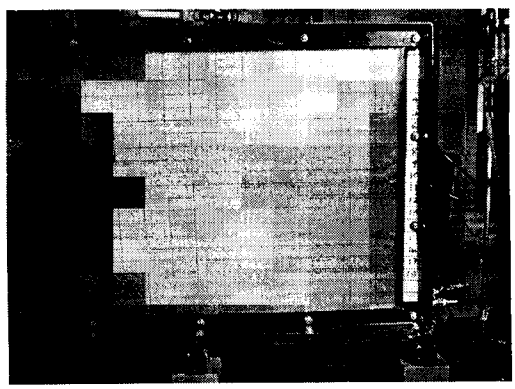

1 hour 19 min

Figure 14: The spill of the TCA in the 2nd experiment

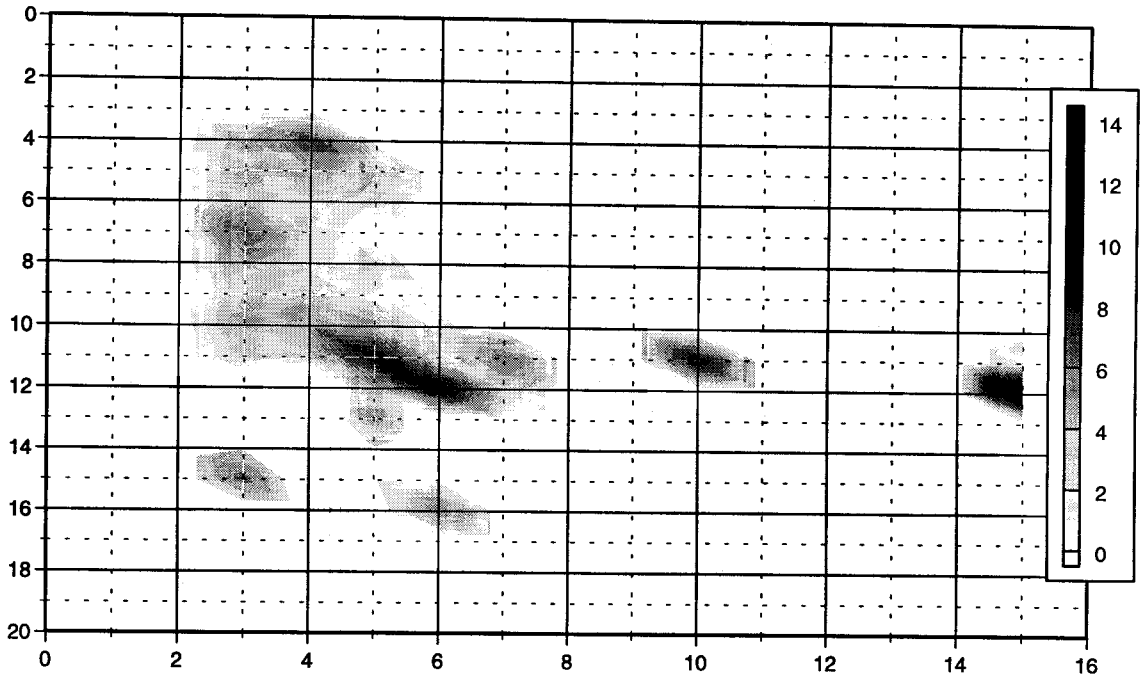

Figure 15: DNAPL saturations one day after the end of the injection of the 2nd experiment.

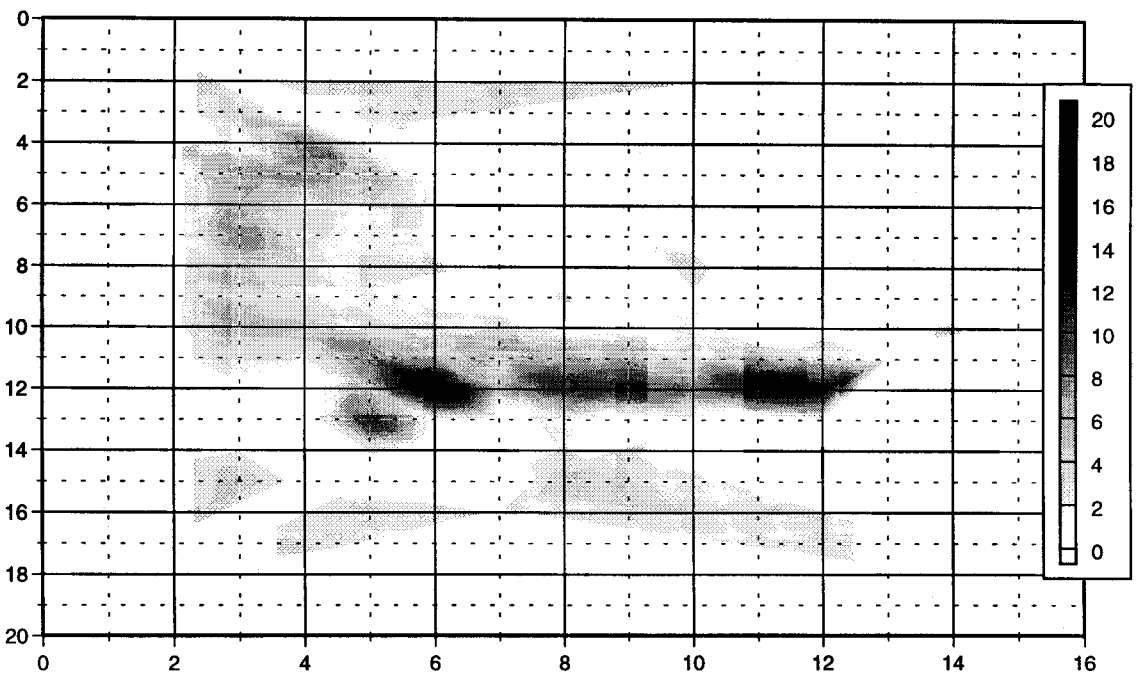

Figure 16: DNAPL saturations three days after the end of the injection of the 2nd experiment.

	1	2	3	4	5	6	7	8	9	10	11	12	13	14	15	16
1		X	X	X	X	X	X									
2		X	X	X	X	X	X									
3		X	X	X	X	X	X									
4		X	X	X	X	X	X									
5		X	X	X	X	X	X									
6		X	X	X	X	X	X	X	X	X						
7		X	X	X	X	X	X	X	X	X	X	X	X			
8		X	X	X	X	X	X	X	X	X	X	X	X			
9		X	X	X	X	X	X	X	X	X	X	X	X	X		
10		X	X	X	X	X	X	X	X	X	X	X	X	X	X	
11		X	X	X	X	X	X	X	X	X	X	X	X	X	X	X
12		X	X	X	X	X	X	X	X	X	X	X	X	X	X	X
13		X	X	X	X	X	X	X	X	X	X	X	X	X	X	X
14		X	X	X	X	X	X	X								
15		X	X	X	X	X	X	X								
16		X	X	X	X	X	X									
17		X	X	X	X											
18		X	X	X	X											
19		X	X	X	X											

Figure 17: With X are marked the locations in the tank, where γ-rays scans were performed during the 2nd experiment.